EUROPEAN COMMISSION

Community Research

SEVENTH FRAMEWORK PROGRAMME

ARCHER

Collaborative Project

Co-funded by the European Commission under the
Euratom Research and Training Programme on Nuclear Energy
within the Seventh Framework Programme

Grant Agreement Number: 269892
Start date: 01/02/2011 Duration: 48 Months

www.archer-project.eu

Advanced Reactor for Cogeneration of Heat & Electricity-R&D

Reports on graphite selection and recommended design properties.

Part II - results for the 950°C INNOGRAPH irradiation experiments (2A and 2B)

Deliverable D41.17

M W Davies (AMEC)

ARCHER project – Contract Number: 269892
Advanced High-Temperature Reactors for Cogeneration of Heat and Electricity R&D
EC Scientific Officer: Dr. Panagiotis Manolatos

Document title	Reports on graphite selection and recommended design properties. Part II - results for the 950°C INNOGRAPH irradiation experiments (2A and 2B)
Author(s)	M W Davies (AMECFW)
Number of pages	39
Document type	Report
Work Package	WP41
Document number	D41.17
Issued by	AMEC
Date of completion	29/01/15
Dissemination level	Restricted to the partners of the ARCHER project

Summary

This document contains the assessment of the 950°C graphite irradiation experiments INNOGRAPH 2A and 2B. The assessment looks at the dimensional change behaviour of the graphites tested, along with the changes in dynamic Young's modulus, coefficient of thermal expansion and thermal conductivity. In terms of properties, the assessment shows that all the graphites behave qualitatively in the same way, and in a similar way to graphites irradiated in the past. However, there are significant differences in the dimensional change behaviour of the different graphites, which is the most important attribute from a core design point of view. There were large differences between the extruded and vibro-moulded graphites and the iso-moulded graphites. This was attributed to the difference in grain size rather than the manufacturing method. The extruded and vibro-moulded graphites had a medium grain size (2mm down to 0.7mm), whereas the iso-moulded graphites had a fine to super-fine grain size (0.1mm down to 5µm). There were also significant differences found between the with-grain (WG) and against-grain (AG) directions, which was not expected for some graphites.

In terms of dimensional change behaviour, the critical factors are the rate of initial shrinkage, the peak shrinkage (i.e. at turn-around), the fluence at which this occurs, and the fluence at which cross-over occurs, which is when the dimensions/volume return to their pre-irradiation values. For any particular graphite, this is considered to be the limiting fluence for the core as it is impractical to design a core structure which can accommodate significant, if any, nett growth. For the graphites tested, the fluence for cross-over ranges from 7.0 dpa to 9.4 dpa for the AG direction, and 8.0 dpa to 11.2 dpa for the WG direction.

Approval

Rev.	Short description	First author	WP Leader	Domain leader	Coordinator
0	First issue	M W Davies .(AMEC)	A Vreeling (NRG)	D Buckthorpe (AMEC)	S Knol (NRG)

Distribution list

Name	Organisation	Comments
P. Manolatos	EC DG RTD	
All technical participants	ARCHER	
Steering Committee members	ARCHER	

DOCUMENT ISSUE RECORD
(engineering documents)

Document Title :	**Reports on graphite selection and recommended design properties. Part II - results for the 950°C INNOGRAPH irradiation experiments (2A and 2B)**
Project Reference:	100525

Purpose of Issue : Issue to client

Security Class : Not protectively marked

Issue	Description of Amendment	Originator/ Author	Checker	Approver	Date
01	First Issue	M W Davies	D Buckthorpe	J O'Keefe	Jan 2015

Total number of pages:	Intro:		Text	37	Tables		Figures		Appendices	

Previous issues of this document shall be destroyed or marked **SUPERSEDED**

Distribution: ARCHER partners, M W Davies, D Buckthorpe, A Grainger

3050aDec07 Controlling Procedure ProcessNet 9.7.1

Table of contents

1 Introduction & Scope

In order to support the development of a future European High Temperature Reactor (HTR), a number of candidate graphites were selected for an irradiation programme, referred to as INNOGRAPH. This programme was undertaken by NRG using the high flux reactor (HFR) at Petten and was aimed at establishing the irradiation behaviour of selected graphites over the fluence and temperature range appropriate for a HTR. This would indicate the 'best' graphite(s) to be selected and would provide a significant amount of the data necessary to undertake a graphite core design.

Based on the reference design for the Pebble Bed Modular Reactor (PBMR) at the time, the peak fluence to be achieved for the irradiation programme was set at 25 displacements per atom (dpa), i.e. ~200 x 10^{20} n.cm^{-2} Equivalent DIDO Nickel Dose (EDND), and the temperature range was set at 550°C to 950°C. It was decided to carry out the first irradiation experiment at the mid-point of the temperature range i.e. 750°C, and in two phases. The first phase, referred to as INNOGRAPH 1A (Refs 1 and 2), was carried out within the 5th Framework Programme (HTR-M1) to a maximum fluence of ~1/3 of the target peak fluence, i.e. 8-9 dpa (~65-70 x 10^{20} n.cm^{-2} EDND). The second phase, referred to as INNOGRAPH 1B (Refs 3 and 4), was carried out in the 6th Framework Programme (RAPHAEL), to a maximum fluence of ~ 2/3 of the target peak fluence, i.e. 15-16 dpa (~125-130 x 10^{20} n.cm^{-2} EDND). After the PIE of the INNOGRAPH 1A samples had been carried out, around half of the samples were placed in the INNOGRAPH 1B experiment, the remaining positions being filled with fresh graphite samples. With this arrangement, the fresh samples would see ~2/3 of the peak fluence and the samples previously irradiated in INNOGRAPH 1A would be irradiated up towards the peak fluence. Due to the flux buckling of the HFR, each experiment would see a range of fluences, with the samples at the top and bottom seeing about 0.65 of the fluence in the centre. In both cases, a full post-irradiation examination (PIE) of the samples was carried out. This involved measuring their new dimensions and mass (from which their new volumes and densities were calculated) as well as dynamic Young's modulus (DYM), coefficient of thermal expansion (CTE) and thermal diffusivity (from which their thermal conductivity was calculated). In addition, another irradiation experiment was carried out in ARCHER at 750°C, but this time only to a fluence of ~1-2 dpa (~12-25 x 10^{20} n.cm^{-2} EDND). This was aimed at getting a better understanding of the variation in some properties that change rapidly over the first 1-2 dpa of irradiation. This was referred to as INNOGRAPH 1C (Ref 5) and the full PIE of the samples is reported in Ref 6. The results of the INNOGRAPH 1A, 1B and 1C experiments are assessed in a companion report to this report, Ref 7.

Another two irradiation experiments, referred to as INNOGRAPH 2A and 2B, were also carried out in the 6th Framework Programme (Refs 8 and 9). These are the equivalent of INNOGRAPH 1A and 1B, but at a temperature of 950°C. This was selected because there was a move towards the development of a Very High Temperature Reactor (VHTR), in which the graphite temperatures would be significantly higher than for the HTR. The peak fluence to be achieved was set at only 14 dpa (~120 x 10^{20} n.cm^{-2} EDND) because the higher temperature would result in a lower fluence to dimensional change turnaround and to positive growth (cross-over), which is a limiting feature of the capsule design. The PIE of all the specimens was carried out within ARCHER and the assessment of the data, including dimensional change, DYM, CTE and thermal conductivity is carried out in this report. A summary of the graphites grades/samples tested is given in Section 2. The pre-characterisation of the graphites and the PIE measurements are covered in Section 3. The dimensional change behaviour with irradiation fluence for each graphite is covered in Section 4. The DYM changes are covered in Section 5, the CTE changes in Section 6 and the thermal conductivity changes in Section 7. [Note - Another companion report to this report, Ref 10, looks at all the INNOGRAPH data. It discusses graphite selection and recommends design 'curves' for property variations].

2 Graphite grades/samples

There is clearly a limit on the number of samples that can be contained within a given irradiation experiment, and as there is a need to maximise the number of samples of each graphite selected to provide good statistics, this had an influence on the number of graphites that can be tested. Another important consideration is that the general anisotropy of the different graphites requires samples to be machined from the two major directions, that is, 'with grain' (WG) and 'against grain' (AG). In addition, due to the inherent material variability within a block, samples should be taken from both the centre region of a block and from the outside region of the block (hereafter referred to as 'centre' and 'edge' in this report).

In keeping with the INNOGRAPH 1A and 1B experiments (assessed in Ref 1), the same candidate graphites from 3 manufacturers were chosen for INNOGRAPH 2A and 2B, with the exception of NBG-20, which was dropped for a number of reasons. These cover the two main sources of coke (petroleum and pitch), and the two most common manufacturing techniques (extrusion and iso-moulding). Two additional grades (NBG-18 and NBG-17) were added to cover another manufacturing technique, namely, vibro-moulding. A third grade was also added (LPEB/BAN) because it exhibited the lowest anisotropy with regard to dimensional change behaviour of any graphite previously tested. The ten selected grades are listed in Table 1. Five of these were classified as 'major' grades, and the other five were classified as 'minor' grades. It should be noted that a small number of graphites were interchanged after the INNOGRAPH 1A experiment between 'major' and 'minor' and vice versa. Again, there was a mixture of two sample lengths (6 mm and 12 mm).

Manufacturer	Grade	Coke	Grain size	Process	Classification
GrafTech	PCEA	Petroleum	Medium	Extrusion	Major
	PPEA	Pitch	Medium	Extrusion	Major
	PCIB-SFG	Petroleum	Super-fine	Iso-moulding	Minor
	LPEB/BAN	Petroleum	Medium	Extrusion	Minor
SGL	NBG-10	Pitch	Medium	Extrusion	Major
	NBG-25	Petroleum	Fine	Iso-moulding	Minor
	NBG-18	Pitch	Medium	Vibro-moulding	Major
	NBG-17	Pitch	Medium	Vibro-moulding	Minor
Toyo Tanso	IG-110	Petroleum	Fine	Iso-moulding	Minor
	IG-430	Pitch	Fine	Iso-moulding	Minor

Table 1 – Selected graphites for the INNOGRAPH 2A and 2B irradiation experiment

3 Pre-characterisation and post-irradiation measurements

3.1 Pre-characterisation measurements

The graphite blocks supplied by the manufacturers for each grade were sectioned and machined to produce the required number of samples. Each sample was cylindrically shaped with a nominal diameter of 8 mm and a nominal length of 6 or 12 mm. As mentioned earlier, the samples were machined from both the central and outer regions of each block, to take account of the known variability in properties throughout it. In addition, a small flat was also machined on each sample so that it could be uniquely identified with an alphanumeric code, and its orientation within the block would be known for recording the measurements (Figure 1). In this way, initial property variations as a function of position and orientation in the block, could be determined (as well as for the irradiated properties).

The dimensions of each sample (see Section 3.2) were measured together with its DYM, CTE and thermal diffusivity (used to calculate thermal conductivity). The mass of each sample was also measured, which together with the dimensions, allowed the initial density to be determined. Details of the testing methods used are given in Ref 1. All the measurements (together with specific properties derived from them) were recorded in an Excel spreadsheet developed by NRG.

[Note - Although strength is a very important property from a core design point of view, it cannot be measured on the samples to be irradiated as this will involve a destructive test. Nevertheless, strength measurements can be made on other suitable samples obtained from a disc/block, and the strength distribution thus obtained should be representative of those being irradiated. Measurements of non-irradiated and irradiated strength were carried out within the ARCHER programme and the results are reported in Ref 10. All show the typical behaviour, which is an initial sharp increase at low fluence, followed by a plateau and then a further rise to a peak, after which it continues to fall.

3.2 Sample Orientations

Given the need to cover both principal directions (WG and AG), the cylindrical shape of the samples with the machined flat meant that great care had be used to ensure that the principal directions were maintained for each sample during manufacture. Figure 2 shows the orientations of the samples taken from both an extruded block and an iso-/vibro-moulded block. It can be seen that the extruded block has one principal WG direction and two principal AG directions, whereas the iso-/vibro-moulded block has two principal WG directions and one principal AG direction. The figure also shows the three dimensions measured, namely the axial length (L), the major diameter (D) and the smaller diameter perpendicular to the flat (X). The samples are classified as WG or AG according to the axial direction, hence the axial length L is always in this (assigned) orientation. The classification of the other two dimensions however depends on its orientation and also which type of block it came from. Table 2 below gives the appropriate classifications.

Process	**Sample orientation**	**Classification**		
		L	**D**	**X**
Extrusion	WG	WG	AG	AG
	AG	AG	AG*	WG*
Iso-moulding, Vibro-moulding	WG	WG	WG*	AG*
	AG	AG	WG	WG

Table 2 – Classification of sample dimensions with respect to sample orientation

* These classifications rely on the flat being machined with the sample in (or very close to) the correct orientation. If this was not the case for any sample, these particular measurements will not be 100% WG or AG, but will be somewhere in between, and this would reduce their usefulness.

3.2 Post-irradiation examination measurements

All the measurements carried out for the pre-characterisation are also required on the irradiated samples (i.e. dimensions, mass, DYM, CTE and thermal diffusivity). All PIE measurements (together with specific properties derived from them) have been added alongside the pre-characterisation measurements in the Excel spreadsheets developed by NRG.

3.3 Assessment spreadsheet

As stated earlier, the INNOGRAPH experiments were aimed at establishing the irradiation behaviour of selected graphites over the fluence and temperature range appropriate for a HTR. This would allow the 'best' graphite(s) to be selected and would provide a significant amount of the data necessary to undertake a graphite core design. To faciltate this, a spreadsheet was developed by AMEC which arranges all the data in a convenient way that enables the appropriate material property behaviour 'curves' to be produce for each. The pre-characterisation data for each graphite were simply copied from the NRG spreadsheet to the first part of the individual worksheet for each grade (Figure 3) and the PIE data were copied to the second part (Figure 4). The third part of the spreadsheet (Figure 5) calculates the changes in the property, either expressed as a percentage change (dimensions and volume), or a fractional change (DYM, CTE and thermal conductivity). The AMEC spreadsheets are used to produce plots of the changes to individual dimensions (L, D and x), volume, DYM, CTE and thermal conductivity. The plots illustrate the difference between the WG and AG behaviour (anisotropy), the scatter in the behaviour, and any differences between 'centre' and 'edge' samples for each direction can be determined if needed.

In Sections 4 to 7 of this report, the dimensional change behaviour and the variations in DYM, CTE and thermal conductivity are assessed for the 4 'major' graphites, namely NBG10, NBG 18, PCEA, and PPEA, as well as 'minor' grade NBG25.. The other 'minor' grades, namely, PCIB, NBG17, IG-110, IG-430 and LPEB/BAN are not assessed due to the limited amount of data.

4 Dimensional change behaviour due to irradiation

The irradiation behaviour of the 5 INNOGRAPH 2A & 2B graphites in terms of the linear dimensional changes for the WG and AG directions, and the volumetric changes are given in Figures 6 to 10. The plots are all shown over the same ranges (-4.0% to +12.0% for dimensional change and -10% to +35% for volumetric change) to give an easier visual comparison of the different behaviours. A negative value indicates shrinkage/volume reduction and a positive value indicates that there is a nett growth/volume increase relative to the unirradiated values. Second order equations (trendlines) generated by Excel have been fitted to the data where appropriate. (For the 750^{o}C data assessed in Ref 7, it was possible to fit fourth order equations, because of the additional low fluence data, which appear to confirm previous suggestions that the dimensional change and volume change rates at low fluences are much smaller than at higher fluences). The behaviour of each graphite is covered in Sub-sections 4.1 and 4.2 below in terms of manufacturer. A discussion on the specific differences and similarities between the behaviour of the different grades is given in Sub-section 4.5.

4.1 SGL grades

For NBG-10, which is a pitch coke extruded graphite, it can be seen from Figure 6a that there is some anisotropy with regard to dimensional change. The maximum average shrinkage is -1.5% (at 6.0 dpa) in the WG direction. This is larger than that for the AG direction, which is -1.0% (at 5.5 dpa). The larger shrinkage and later turnaround for the WG direction results in a slightly higher fluence to (average) cross-over, being 9.1 dpa for the WG direction compared to 8.2 dpa for the AG direction. The delay also means that the maximum growth reached at the end of the experiment for the WG direction, at +4.8%, is less than for the AG direction, at +7.5%. There is also quite a lot of scatter in the data at the higher fluences. The volume change behaviour is shown in Figure 6b. It can be seen that the maximum volume shrinkage is -3.7% (at 5.5 dpa). The average cross-over point occurs at 8.4 dpa and the average maximum volume growth at the peak fluence is +22.5%. The scatter for volume is clearly less than that for the dimensions up to the cross-over point, but thereafter it is broadly similar.

For NBG-18, which is a pitch coke vibro-moulded graphite, it can be seen from Figure 7a that there is a similar anisotropy with regard to dimensional change to that for NBG-10. The maximum average shrinkage is -1.4% (at 4.5 dpa) in the WG direction. This is larger than that for the AG direction, which is -1.1% (at 4.0 dpa). The slightly larger shrinkage and later turnaround for the WG direction results in a slightly higher fluence to (average) cross-over, being 8.0 dpa for the WG direction compared to only 7.2 dpa for the AG direction. The delay also means that the maximum growth reached at the end of the experiment for the WG direction, at +6.2%, is slightly less than for the AG direction, at +7.4%. The volume change behaviour is shown in Figure 7b. It can be seen that the maximum volume shrinkage is -5.0% (at 4.0 dpa). The average cross-over point occurs at 8.0 dpa and the average maximum volume growth at the peak fluence is +25.5%. The scatter for volume is clearly less than that for the dimensions. The scatter at higher fluence is less than that for NBG10.

For NBG-25, which is a petroleum coke iso-moulded graphite, it can be seen from Figure 8a that there is a larger anisotropy with regard to dimensional change than for NBG-10 and NBG-18, which would not be expected. The maximum average shrinkage is -0.9% (at 6.0 dpa) in the WG direction. This is much larger than that for the AG direction, which is only -0.5% (at 4.0 dpa). The larger shrinkage and much later turnaround for the WG direction results in a much higher fluence to (average) cross-over, being 9.6 dpa for the WG direction compared to only 7.0 dpa for the AG direction. The delay in turnaround also means that the maximum growth reached at the end of the experiment for the WG direction, at +3.5%, is less than for the AG direction, at +6.8%. The volume change behaviour is shown in Figure 8b. It can be seen that the maximum volume shrinkage is -2.5% (at 5.0 dpa). The average cross-over point occurs at 8.6 dpa and the average maximum volume growth at the peak fluence is +14.2%. The scatter for volume is clearly less than that for the dimensions. The scatter at higher fluence is less than that for both NBG-10 and NBG-18.

Grade	Dimensional change - AG				Dimensional change - WG				Volume change			
	Maximum shrinkage	dpa to turn-around	dpa to cross-over	Maximum growth	Maximum shrinkage	dpa to turn-around	dpa to cross-over	Maximum growth	Maximum shrinkage	dpa to turn-around	dpa to cross-over	Maximum growth
NBG-10	-1.2	4.5	8.0	8.0	-1.6	5.0	9.0	5.3	-4.0	5.0	8.3	24.5
NBG-18	-1.1	4.0	7.2	7.4	-1.4	4.5	8.0	6.2	-5.0	4.0	8.0	25.5
NBG-25	-0.5	4.0	7.0	6.8	-0.9	6.0	9.6	3.5	-2.5	5.0	8.6	14.2
PCEA	-1.4	6.0	9.4	7.0	-2.3	7.0	11.2	4.0	-5.0	6.5	9.9	20.0
PPEA	-1.0	5.0	8.0	10.0	-1.8	6.0	9.9	6.9	-3.6	5.5	8.6	30.0

Table 3 – Summary of dimensional changes and volume changes

4.2 GrafTech graphites

The GrafTech grades also cover both petroleum and pitch coke, and both extrusion and iso-moulding. For PCEA, which is a petroleum coke, extruded graphite, it can be seen from Figure 9a that there is some anisotropy with regard to dimensional change. The maximum average shrinkage is -2.3% (at 7.0 dpa) in the WG direction. This is larger than that for the AG direction, which is -1.4% (at 6.0 dpa). The larger shrinkage and later turnaround for the WG direction results in a higher fluence to (average) cross-over, being 11.2 dpa for the WG direction compared to 9.4 dpa for the AG direction. The delay in turnaround also means that the maximum dimensional change reached at the end of the experiment for the WG direction is much less than for the AG direction. For the former, there is a growth of +4.0%, whereas for the latter there is a growth of +7.0%. The volume change behaviour is shown in Figure 9b. It can be seen that the maximum volume shrinkage is -5.0% (at 6.5 dpa). The average cross-over point occurs at 9.9 dpa and the average maximum volume growth at the peak fluence is +20%. The scatter for volume is clearly less than that for the dimensions up to the cross-over point, but thereafter it is larger, but not as large as the scatter for dimensions.

For PPEA, which is the pitch-coke-equivalent of PCEA (and also the equivalent grade to NBG-10), it can be seen from Figure 10a that there is again some anisotropy. The maximum average shrinkage in the WG direction is -1.8% (at 6.0 dpa). This is larger than in the AG direction, which is -1.0% (at 5.0 dpa). The larger shrinkage and later turnaround for the WG direction results in a higher fluence to (average) cross-over, being 9.9 dpa for the WG direction compared to 8.0 dpa for the AG direction. The delay also means that the maximum dimensional change reached at the end of the experiment for the WG direction is much less than for the AG direction. For the former, there is growth of +6.9%, whereas for the latter there is a growth of +10.0%. The volume change behaviour is shown in Figure 10b. It can be seen that the maximum volume shrinkage is -3.6% (at 5.5 dpa). The average cross-over point occurs at 8.6 dpa and the average maximum volume change at the peak fluence is +30%. The scatter is slightly less than for the individual dimensions.

4.3 Discussion

It can be seen that all of the graphites tested show the same qualitative dimensional change behaviour, whereas there is a significant different in the quantitative behaviour between the different grades. Table 3 gives a summary of the important measures of dimensional change behaviour from a core design point of view, namely the peak shrinkages reached at turn-around (for both WG and AG directions), the fluences at which these occur, and the fluences at which the original dimensions and volumes are reached (cross-over). The maximum dimensional and volume growths at the peak fluences attained are also given, although these are more of an academic interest as any realistic core designs will not be able to accommodate any significant nett growth, and so the cross-over point would be the general fluence limit applied.

As a general observation, it could be seen that the AG direction for all the graphites exhibited less shrinkage than the WG grain direction. However, a consequence of this was that the AG direction always exhibited turn-around at a lower fluence than the WG direction and also reached cross-over at a lower fluence. For the AG direction, it can be seen from Table 3 that the maximum shrinkage attained was -1.4% (for PCEA), and this occurred at the highest fluence (6.0 dpa). This graphite also had the highest fluence to reach cross-over (9.4 dpa), which would be expected given it had the highest fluence to turn-around. The minimum shrinkage was -0.5% (for NBG-25) and this occurred at the lowest fluences (4.0 dpa) although NBG-18 also reached its maximum shrinkage at this fluence. NBG-25 had the lowest fluences to reach cross-over (7.0 dpa), slightly ahead of that for NBG-18 (7.2 dpa).

For the WG direction, it can be seen from Table 3 that the maximum shrinkage was again attained by PCEA (-2.3%), which occurred at the highest fluence of 7.0 dpa. It also had the highest fluence to reach cross-over (11.2 dpa). The minimum WG shrinkage was -0.9% (for NBG-25) which occurred at a fluence of 6.0 dpa. The graphite the lowest fluence to reach a minimum shrinkage was NBG-18 (at 4.5 dpa), which also had the lowest fluence to cross-over (8.0 dpa).

In terms of volume change, it can be seen from Table 3 that the maximum volume shrinkage was again attained by PCEA (-5.0%), which occurred at the highest fluence of 6.5 dpa. PCEA had the highest fluence to reach volume cross-over (9.9 dpa). NBG-18 also had a maximum volume shrinkage of -5.0% but this occurred at the lowest fluence (of 4.0 dpa). It also had the lowest fluence to cross-over (8.0 dpa). The minimum volume shrinkage was attained by NBG-25, but this had a higher fluence to turnaround (5.0 dpa) and cross-over (8.6 dpa) than NBG-18.

5 Dynamic Young's modulus

The variation in DYM with irradiation fluence for the 5 graphites is given in Figures 11 to 15. Figures 11a to 15a show the actual variations and Figures 11b to 15b show these as a fractional change, or multiplying factor (expressed as DYM_{irr}/DYM_{unirr}). All 5 graphites show the familiar trend seen for all graphites irradiated in the past. Although not evident from the data, there is an initial very sharp increase in DYM over a fluence range of 0-1 dpa. This is attributed to the pinning of mobile dislocations in the lattice structure. (In the UK this is referred to as the 'pinning' term). A short plateau then have been reached, again not evident, which continues up to around 3 dpa. At progressively higher fluences there is a further, but more gradual, increase in DYM attributed to structural changes within the crystals. (In the UK this is referred to as the 'structure' term.). A peak value is then reached, and thereafter, the DYM decreases fairly rapidly thereafter as the graphite structure begins to break down.

Table 4 below summarises the initial DYM increase factor for each graphite and also the peak factor along with the approximate fluence when this is reached. Unlike the assessment carried out on the 750^{o}C (Ref 7), which had the benefit of the low fluence data, it was not possible to get an accurate value for the initial factorial increase. The data for NBG-10, NBG-18 and PCEA suggest that the second increase in DYM is just beginning (i.e. the plateau has just ended) and so the initial increases are by a factor of between 1.4 and 1.5. For the other two graphites, it looks as if the data are well into the second increase phase. When the peak DYM is reached, the three pitch coke graphites (NBG-10, NBG-18 and PPEA) have increased by a factor of around 2.75, whereas the two petroleum coke graphites have increased by a factor of between 3.33 and 3.40. This is a very interesting observation as the increase appears to be related to the coke rather than to the grain size. If it had been related to grain size, the PCEA factorial increase would have been closer to 2.75, which is the value for the medium grain graphites. The fluence at which the peak DYM is reached is consistent across all five graphite types i.e. ~8 dpa. After the peak value is reached the DYM continues to decrease fairly rapidly thereafter as the graphite structure begins to break down. (It should be noted that the strength of graphite also increases with fluence in a similar way to the DYM. Both factorial increases, however, will be generally less than those for DYM).

Graphite	Type	Initial multiplying factor	Maximum multiplying factor	Fluence at which peak DYM is reached
NBG-10	Extruded	1.5	2.73	~8
PPEA	Extruded	-	2.75	~8
NBG-18	Vibro-moulded	1.4	2.75	~8
PCEA	Extruded	1.4	3.33	~8
NBG-25	Iso-moulded	-	3.40	~8

Table 4 – Multiplying factors for the increases in DYM

6 Coefficient of thermal expansion

The variation in CTE with irradiation fluence for the 5 graphites is given in Figures 16 to 20. Figures 16a to 20a show the actual variations and Figures 16b to 20b show these as a fractional change, expressed as $(CTE_{irr} / CTE_{unirr}) - 1$, which is the customary way of doing this. Each plot shows the value of the mean CTE over 4 temperature ranges, 30-120^{o}C, 30-200^{o}C, 30-750^{o}C and 30-950^{o}C. All 5 graphites show the familiar trend seen for all graphites irradiated in the past. Unlike the assessment carried out on the 750°C (Ref 7), which had the benefit of the low fluence data, it was not possible to see the initial small increase at the lower fluences. Nevertheless, it can be assumed that this small initial increase did occur, after which there is a progressive decrease until a plateau is reached, which is evident from the data. As the fluence increases further, there are differences in behaviour between the different graphites. For the petroleum coke graphite (NBG-25), there appears to be a further decrease in CTE with increasing fluence, whereas for the pitch coke graphites, the CTE appears to be increasing. This is a very interesting observation.

7 Thermal conductivity

The variation in thermal conductivity with irradiation fluence for the 5 graphites is given in Figures 21 to 25. Figures 21a to 25a show the actual variations and Figures 21b to 25b show these as a fractional change, expressed as $(TCon_{irr} / TCon_{unirr}) - 1$, which is the customary way of doing this. Each plot shows the value of the instantaneous thermal conductivity at temperatures of 27, 100, 200, 300, 400, 500, 600, 700, 800, 900 and 950°C. It can be seen from Figures 21a to 25a that the thermal conductivity of each graphite decrease with increasing temperature. When irradiated, all 5 graphites show the familiar trend seen for all graphites irradiated in the past. Unlike the assessment carried out on the 750°C (Ref 7), which had the benefit of the low fluence data, it was not possible to see the initial very large reduction in thermal conductivity at the lower fluences (0-2 dpa range). Nevertheless, it can be assumed that this rapid decrease in thermal conductivity did occur, after which a plateau is reached, which is evident from the data. At higher fluences, a further decrease in thermal conductivity is observed, and this is consistent with the behaviour of other graphites irradiated in the past.

8 Conclusions

This document contains the assessment of the 950°C graphite irradiation experiments INNOGRAPH 2A and 2B. The assessment looks at the dimensional change behaviour of the graphites tested, along with the changes in DYM, CTE and thermal conductivity. In terms of properties, the assessment shows that all the graphites behave qualitatively in the same way, and in a similar way to graphites irradiated in the past. However, there are significant differences in the dimensional change behaviour of the different graphites, which is the most important attribute from a core design point of view. There were large differences between the extruded graphites, the iso-moulded graphites and the vibro-moulded graphites. This was attributed to the difference in grain size rather than the manufacturing method. The extruded and vibro-moulded graphites had a medium grain size (2mm down to 0.7mm), whereas the iso-moulded graphites had a fine to super-fine grain size (0.1mm down to 5µm). There were also significant differences found between the with-grain (WG) and against-grain (AG) directions, which was not expected for some graphites.

In terms of dimensional change behaviour, the critical factors are the rate of initial shrinkage, the peak shrinkage (i.e. at turn-around), the fluence at which this occurs, and the fluence at which cross-over occurs, which is when the dimensions/volume return to their pre-irradiation values. For any particular graphite, this is considered to be the limiting fluence for the core as it is impractical to design a core structure which can accommodate significant, if any, nett growth. For the graphites tested, the fluence for cross-over ranges from 7.0 dpa to 9.4 dpa for the AG direction, and 8.0 dpa to 11.2 dpa for the WG direction..

9 References

1 F. Schmalz et al. Preliminary irradiation testing of selected graphite grades for HTR, Final report on HTR-M1 WP3, 20787/05.71179/P, 19 December 2005

2 J.A. Vreeling, B. Sakintuna. DML3.13: Full PIE of INNOGRAPH-1A and description of INNOGRAPH-1B, NRG-21457/10.101850, 14 April 2010

3 O. Wouters, J.A. Vreeling. INNOGRAPH-1B and INNOGRAPH-2A specimen manufacture and pre-characterisation, DML3.3: Graphite material procurement & characterisation, 21457/06.77300/P, 23 October 2006

4 M Henjia. High Dose. Experiments at 750℃ & 950℃ - Full PIE of INNOGRAPH-IB and INNOGRAPH-2B. ARCHER deliverable D41.12:

5 M Heijna. Final design proposal for the low dose irradiation experiment INNOGRAPH 1C. ARCHER deliverable D41-13

6 M Heijna. PIE report of low dose irradiation experiment at 750ºC, INNOGRAPH 1C. ARCHER deliverable D41-21

7 M W Davies. Reports on graphite selection and recommended design properties- Part II - results for the 750°C INNOGRAPH irradiation experiments (2A and 2B). ARCHER deliverable D41-16

8 O. Wouters, J.A. Vreeling. INNOGRAPH-1B and INNOGRAPH-2A specimen manufacture and pre-characterisation, DML3.3: Graphite material procurement & characterisation, 21457/06.77300/P, 23 October 2006

9 M Heijna. High Dose. Experiments at 750℃ & 950℃ - Full PIE of INNOGRAPH-IB and INNOGRAPH-2B. ARCHER deliverable D41.12:

10 M W Davies. Reports on graphite selection and recommended design properties- Part III – graphite selection and recommended design properties. ARCHER deliverable D41-18

11 M Heijna. Report on strength measurements of irradiated graphite. ARCHER deliverable D41-15

Figure 1 – Sample machining and dimensions

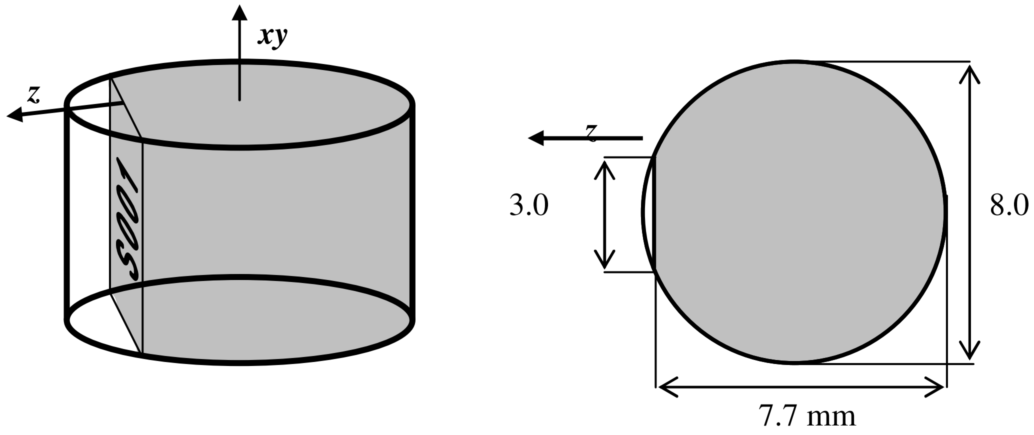

The figure on the left-hand side exaggeratedly shows the machined flat on the side of the cylinder. The milled plane is perpendicular to the *z*-direction when the axial direction of the cylinders in the *xy*-direction. The specimen number is engraved on the plane. The figure on the right-hand side is a top-view of the specimen. The important dimensions are indicated.

Figure 2 - Orientation of dimensions with grain directions

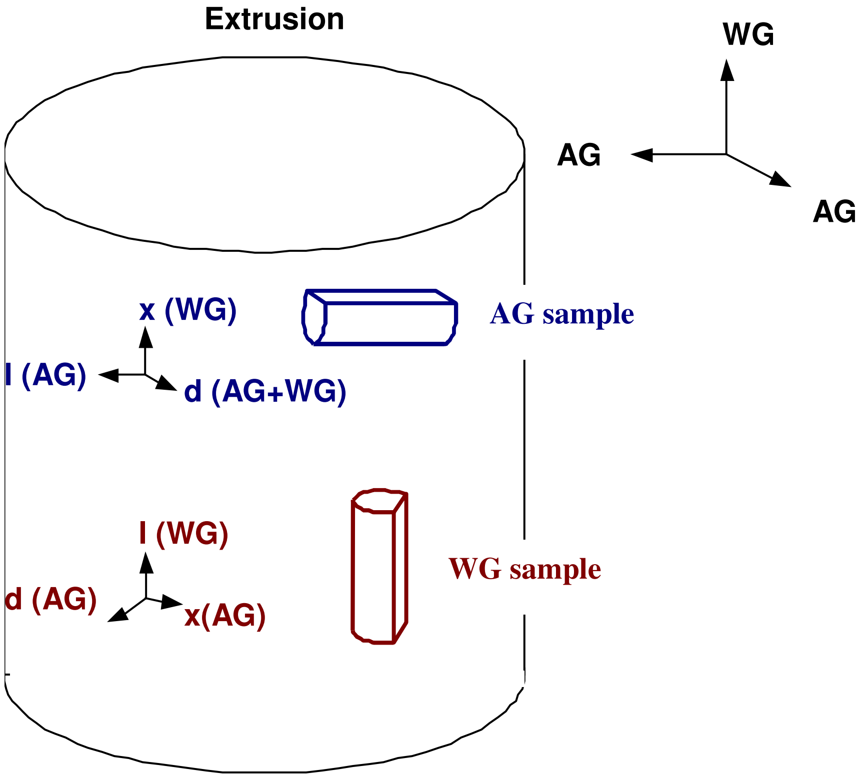

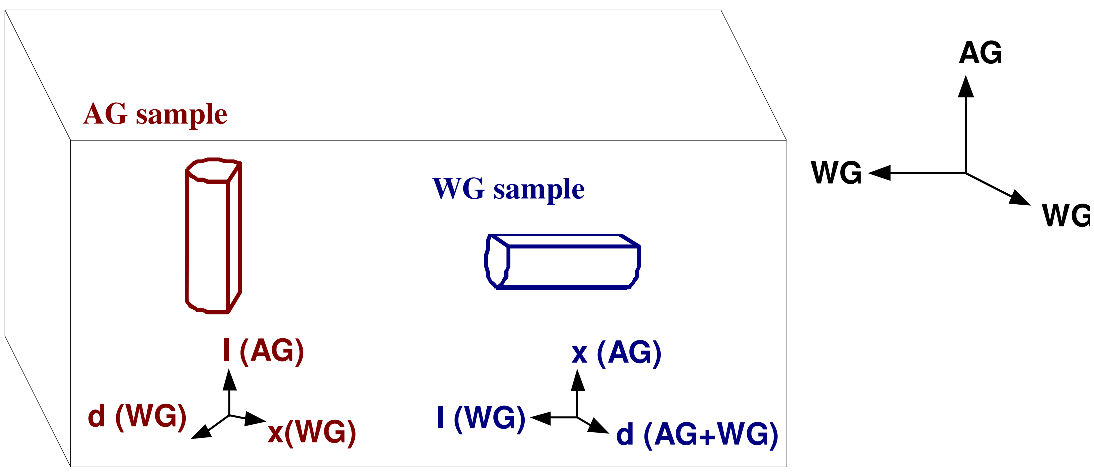

Iso-moulding

Figure 3 – Assessment spreadsheet – unirradiated values

Spec code	Block region	Orient-ation	Unirradiated properties																				
			Length L_o (mm)	Diam D_o (mm)	Diam x (mm)	Vol V_o (mm^3)	Mass Mo (g)	Density ρo (g/cm^3)	DYM	CTE α_o ($x10^{-6}/K$)				Thermal conductivity (W/m/K)										
									E_o (GPa)	30-120	30-200	30-750	30-950	25°C	100°C	200°C	300°C	400°C	500°C	600°C	700°C	800°C	900°C	950°C
S036	CENTRE	WG	6.027	7.992	7.704	298.8	0.53976	1.806	12.8	4.05	4.17	5.08	5.34	148.3	138.1	121.2	110.6	100.2	91.8	84.1	78.1	71.8	67.3	65.9
S372	CENTRE	WG	11.997	7.990	7.694	594.3	1.07997	1.817	13.1	4.20	4.31	5.16	5.39											
S376	CENTRE	WG	6.013	7.987	7.698	297.8	0.53790	1.806	13.3	3.65	3.94	5.05	5.29	148.2	134.3	121.9	110.3	100.1	91.3	84.6	80.4	74.0	70.4	68.7
S378	CENTRE	WG	6.021	7.990	7.700	298.4	0.54224	1.817	13.4	3.81	4.14	5.22	5.46	148.6	138.4	122.3	111.0	99.8	91.9	83.9	77.2	72.5	68.2	65.9
S382	CENTRE	WG	6.038	7.981	7.697	298.7	0.54366	1.820	13.2	3.93	4.25	5.25	5.48	149.1	140.2	125.4	111.2	100.5	92.8	85.0	78.9	73.0	69.5	66.6
S384	CENTRE	WG	6.018	7.984	7.703	298.0	0.54056	1.814	13.5	4.41	4.39	5.24	5.50	146.6	135.5	123.3	108.8	99.2	90.9	84.6	77.0	71.6	66.9	65.1
S386	CENTRE	AG	6.027	7.997	7.687	298.8	0.54070	1.809	12.7	4.20	4.57	5.42	5.67	141.3	130.3	117.4	106.2	95.8	87.7	80.8	74.9	69.2	64.7	62.1
S387	CENTRE	AG	6.013	7.997	7.696	298.3	0.54181	1.816	12.8	4.12	4.35	5.38	5.62	144.8	136.0	122.2	109.2	100.1	91.4	83.8	76.2	71.2	67.3	65.0
S388	CENTRE	AG	6.048	7.992	7.694	299.7	0.54252	1.810	12.8	4.54	4.46	5.33	5.61	146.4	132.4	119.9	107.5	98.3	88.8	81.7	76.3	70.4	65.1	64.0
S389	CENTRE	AG	5.977	7.993	7.697	296.3	0.53749	1.814	12.7	4.22	4.45	5.41	5.64	144.5	132.5	120.4	106.9	98.3	89.4	82.3	76.6	70.9	66.2	64.6
S390	CENTRE	AG	5.971	7.990	7.689	295.7	0.53646	1.814	12.8	4.33	4.43	5.39	5.64	144.6	134.6	119.8	107.9	98.3	88.6	82.2	75.3	71.3	66.2	63.4
S396	CENTRE	AG	11.986	7.995	7.702	594.6	1.07399	1.806	12.5	4.19	4.41	5.35	5.57											
S391	CENTRE	AG	6.030	7.987	7.687	298.4	0.53617	1.797	12.3	5.06	4.92	5.84	6.00	137.5	127.0	112.8	100.3	89.1	83.5	75.6	70.0	64.7	61.3	59.9
S062	EDGE	WG	5.984	7.987	7.648	295.4	0.53701	1.818	13.5	4.27	4.35	5.34	5.58	148.6	137.8	124.5	112.0	102.7	92.9	85.5	78.9	73.5	67.6	66.1
S342	EDGE	WG	11.964	8.000	7.687	593.6	1.08519	1.828	13.7	4.11	4.32	5.23	5.46											
S346	EDGE	WG	6.012	7.999	7.689	298.3	0.53946	1.809	13.5	3.33	3.80	5.04	5.34	144.4	133.2	121.5	108.5	97.7	90.0	83.6	76.7	71.5	66.6	64.6
S348	EDGE	WG	5.994	7.997	7.687	297.2	0.53941	1.815	13.4	4.03	4.28	5.30	5.54	137.6	126.8	115.5	103.8	93.9	86.3	79.8	73.6	68.6	64.2	62.3
S350	EDGE	WG	6.005	7.994	7.688	297.6	0.53025	1.782	13.1	3.61	3.89	5.12	5.40	130.7	120.4	109.4	99.1	90.1	82.5	75.9	70.4	65.8	61.9	60.0
S352	EDGE	WG	5.915	7.990	7.692	293.0	0.53338	1.820	13.6	3.76	4.01	5.19	5.46	147.2	137.3	125.1	111.4	101.7	91.9	86.3	79.3	73.4	68.7	66.9
S354	EDGE	WG	5.962	7.987	7.698	295.3	0.53546	1.814	13.3	3.90	4.13	5.26	5.51	143.0	134.5	122.3	111.2	100.7	92.1	83.9	78.7	72.7	68.6	66.2
S077	EDGE	AG	5.952	7.986	7.702	294.7	0.52752	1.790	13.0	5.22	5.11	6.12	6.42	142.7	135.5	122.5	109.9	100.3	90.7	83.6	77.2	72.1	67.0	64.9
S356	EDGE	AG	6.011	7.990	7.688	297.7	0.54756	1.839	13.4	3.87	4.32	5.45	5.72	146.8	136.0	122.5	110.9	99.3	91.1	84.7	78.2	71.6	66.7	65.3
S357	EDGE	AG	5.979	7.985	7.685	295.8	0.54718	1.850	13.6	4.32	4.52	5.15	5.74	143.3	133.0	115.1	101.9	90.2	85.7	79.0	73.2	67.9	64.0	62.4
S358	EDGE	AG	5.997	7.998	7.691	297.5	0.54351	1.827	13.1	3.91	4.32	5.27	5.52	142.4	134.8	122.6	109.5	99.6	90.5	84.1	77.5	71.5	67.0	65.4
S359	EDGE	AG	6.046	7.986	7.688	299.2	0.55247	1.847	13.5	4.38	4.55	5.14	5.72	145.3	130.8	115.3	99.1	90.9	85.9	78.5	71.6	66.4	62.2	62.0
S360	EDGE	AG	5.952	8.000	7.692	295.4	0.54004	1.828	13.2	3.41	3.87	5.09	5.37	143.8	134.4	121.0	109.2	98.2	89.9	82.3	77.8	71.7	67.0	64.6
S366	EDGE	AG	12.009	8.000	7.708	596.6	1.09496	1.835	13.3	4.38	4.57	5.46	5.66											

Figure 4 – Assessment spreadsheet – irradiated values

Irrad temp (°C)	Fluence		Irradiated properties																					
	DPA	EDND (10E22)	Length L_i (mm)	Diam D_i (mm)	Diam x_i (mm)	Vol V_i (mm^3)	Mass M_i (g)	Density ρ_i (g/cm^3)	DYM E_i (GPa)	CTE α_i (x10^{-6}/K)				Thermal conductivity (W/m/K)										
										30-120	30-200	30-750	30-950	25°C	100°C	200°C	300°C	400°C	500°C	600°C	700°C	800°C	900°C	950°C
950	5.30	40.3	5.919	7.901	7.620	286.926	0.538	1.875	28.182	1.96	2.07	3.18	3.46	46.1	48.7	51.4	51.6	50.3	49.2	48.1	46.6	45.3	44.5	43.6
950	5.90	44.8	11.816	7.925	7.635	576.047	1.079	1.873	32.243	1.58	1.70	2.73	3.00											
950	5.90	44.8	5.916	7.903	7.626	286.967	0.538	1.874	34.714	1.35	1.56	2.75	3.04	42.8	46.2	49.0	49.1	48.3	47.0	45.7	44.1	42.7	41.5	41.2
950	6.70	50.9	5.946	7.948	7.654	291.457	0.541	1.855	30.974	1.48	1.69	2.80	3.08	39.8	43.2	45.8	46.3	45.8	44.8	43.8	42.5	41.5	40.5	40.1
950	5.10	38.8	5.944	7.890	7.619	287.539	0.541	1.883	29.519	1.48	1.87	3.15	3.44	45.4	48.9	51.3	51.6	50.7	49.6	48.2	46.9	46.0	44.6	44.2
950	4.60	35.0	5.939	7.911	7.642	288.848	0.540	1.870	25.102	1.86	1.98	3.14	3.42	45.4	49.2	51.5	51.5	50.1	48.6	46.9	45.4	43.7	41.9	41.6
950	5.90	44.8	5.976	7.918	7.593	290.164	0.540	1.859	26.899	1.93	2.14	3.24	3.52	41.3	44.8	47.3	47.8	47.1	46.0	45.0	43.7	42.4	41.2	40.8
950	6.40	48.6	5.966	7.906	7.586	288.857	0.540	1.870	35.319	1.56	1.70	2.85	3.14	40.1	44.0	46.7	47.3	46.8	45.7	44.6	43.5	42.4	41.5	40.4
950	6.10	46.4	5.992	7.910	7.592	290.504	0.543	1.868	31.948	1.69	1.84	3.02	3.29	41.6	44.7	47.5	47.9	47.2	46.2	45.0	43.8	42.9	41.4	41.6
950	6.70	50.9	5.935	7.906	7.594	287.522	0.535	1.862	35.220	1.25	1.66	2.93	3.19	37.0	40.5	43.1	43.8	43.3	42.9	42.0	41.2	40.3	39.8	39.3
950	4.10	31.2	5.925	7.929	7.615	288.708	0.536	1.857	21.102	2.51	2.64	3.73	4.03	44.4	48.4	50.4	50.3	49.1	47.6	46.1	44.4	42.8	41.4	41.0
950	5.00	38.0	11.852	7.894	7.583	572.452	1.073	1.874	27.896	1.64	1.81	2.94	3.23											
850	3.60	27.4	6.008	7.959	7.655	295.140	0.534	1.809	17.309	3.73	3.95	4.99	5.12	41.9	44.5	46.6	47.0	46.1	44.9	43.5	41.8	40.8		
950	5.60	42.6	5.883	7.880	7.555	282.871	0.536	1.895	35.057	1.33	1.66	2.93	3.22	45.5	48.8	51.6	51.8	51.1	49.5	48.1	46.7	45.3	44.2	43.1
950	6.50	49.4	11.759	7.931	7.634	573.860	1.084	1.889	38.911	1.44	1.53	2.54	2.80											
950	6.70	50.9	5.941	7.929	7.626	289.645	0.538	1.858	30.395	1.50	1.64	2.79	3.08	38.7	41.6	44.1	44.9	44.2	43.0	42.0	40.8	39.4	38.1	37.4
950	6.40	48.6	5.897	7.927	7.622	287.378	0.537	1.869	36.435	1.04	1.21	2.16	2.44	39.6	42.6	45.5	46.0	45.3	44.7	43.3	42.7	41.2	40.0	40.3
950	5.70	43.3	5.898	7.888	7.604	284.907	0.529	1.857	34.760	0.92	1.20	2.49	2.85	43.0	45.7	48.2	49.0	48.3	48.4	48.3	47.7	47.5	47.1	47.9
950	6.40	48.6	5.815	7.920	7.624	282.999	0.532	1.879	36.594	1.62	1.75	2.88	3.18	39.3	43.0	45.5	46.1	45.7	45.2	44.3	43.1	42.1	41.2	40.6
950	6.30	47.9	5.870	7.917	7.645	285.872	0.535	1.872	36.388	1.50	1.69	2.82	3.12	38.5	41.7	44.5	45.3	44.7	43.9	42.9	41.9	40.5	39.4	39.4
950	5.60	42.6	5.771	7.873	7.586	277.656	0.525	1.891	29.976	1.46	1.61	2.75	3.11	49.0	53.8	56.3	56.8	56.0	55.3	54.5	53.8	52.8	52.6	51.7
950	6.20	47.1	5.967	7.905	7.592	288.941	0.546	1.891	30.399	1.95	2.15	3.22	3.50	41.1	45.0	47.5	48.1	47.4	46.5	45.3	44.0	42.9	41.8	41.8
950	6.50	49.4	5.936	7.888	7.575	286.260	0.545	1.905	35.320	1.58	1.71	2.84	3.11	39.8	43.8	46.5	47.1	46.7	45.9	44.8	43.5	42.5	41.4	41.3
950	5.80	44.1	5.934	7.893	7.567	286.232	0.543	1.898	33.906	1.31	1.60	2.86	3.16	40.8	44.2	47.2	47.6	47.1	46.2	45.2	44.3	42.9	42.1	41.6
950	5.60	42.6	5.987	7.876	7.559	287.753	0.550	1.911	33.281	0.76	1.05	2.49	2.87	44.3	47.7	50.3	50.7	49.7	48.4	47.1	45.9	44.2	42.6	42.6
950	4.70	35.7	5.896	7.913	7.602	286.149	0.540	1.886	25.399	1.85	2.03	3.21	3.52	45.8	49.1	51.5	51.8	50.9	49.5	47.6	46.3	45.1	43.5	43.8
950	6.40	48.6	11.926	7.899	7.596	577.024	1.094	1.895	37.908	1.33	1.49	2.62	2.88											

Figure 5 – Assessment spreadsheet – %/fractional changes

Location	Orientation	Fluence		Fractional change																					
		DPA	EDND (10E22)	Length L (%)	Diam D (%)	Diam x (%)	Vol V (%)	Mass M	Density ρ	DYM E (Gpa)	CTE				Thermal conductivity										
											30-120	30-200	30-750	30-950	25°C	100°C	200°C	300°C	400°C	500°C	600°C	700°C	800°C	900°C	950°C
CENT	WG	5.30	40.3	-1.784	-1.1387	-1.0822	-3.9827	-0.0031	0.03828	2.19356	-0.517	-0.503	-0.374	-0.353	-0.689	-0.648	-0.576	-0.533	-0.498	-0.464	-0.428	-0.404	-0.369	-0.339	-0.339
CENT	WG	5.90	44.8	-1.505	-0.8146	-0.7584	-3.0775	-0.0012	0.0305	2.4546	-0.624	-0.605	-0.470	-0.443											
CENT	WG	5.90	44.8	-1.6128	-1.0549	-0.9387	-3.6256	-0.0004	0.03723	2.61912	-0.631	-0.604	-0.455	-0.426	-0.711	-0.656	-0.598	-0.555	-0.517	-0.485	-0.460	-0.452	-0.423	-0.411	-0.401
CENT	WG	6.70	50.9	-1.2446	-0.531	-0.6038	-2.3239	-0.0028	0.02093	2.31629	-0.611	-0.591	-0.463	-0.435	-0.732	-0.687	-0.625	-0.583	-0.541	-0.513	-0.478	-0.449	-0.428	-0.406	-0.391
CENT	WG	5.10	38.8	-1.5534	-1.1425	-1.019	-3.7352	-0.0041	0.03456	2.23076	-0.623	-0.561	-0.399	-0.373	-0.695	-0.651	-0.591	-0.536	-0.496	-0.465	-0.433	-0.406	-0.370	-0.357	-0.336
CENT	WG	4.60	35.0	-1.3047	-0.9246	-0.784	-3.0589	-0.0006	0.03092	1.86519	-0.577	-0.550	-0.399	-0.378	-0.691	-0.637	-0.583	-0.527	-0.495	-0.466	-0.445	-0.411	-0.390	-0.373	-0.361
CENT	AG	5.90	44.8	-0.8414	-0.9878	-1.2216	-2.9022	-0.0022	0.02767	2.11437	-0.541	-0.531	-0.402	-0.378	-0.708	-0.656	-0.597	-0.550	-0.509	-0.475	-0.443	-0.417	-0.388	-0.363	-0.344
CENT	AG	6.40	48.6	-0.7902	-1.135	-1.4256	-3.1663	-0.0029	0.02971	2.75303	-0.620	-0.610	-0.470	-0.442	-0.723	-0.676	-0.618	-0.567	-0.532	-0.500	-0.468	-0.429	-0.404	-0.382	-0.378
CENT	AG	6.10	46.4	-0.9235	-1.02	-1.3253	-3.0777	4.3E-05	0.0318	2.49516	-0.627	-0.588	-0.434	-0.414	-0.716	-0.662	-0.604	-0.554	-0.520	-0.480	-0.449	-0.426	-0.391	-0.365	-0.351
CENT	AG	6.70	50.9	-0.701	-1.0923	-1.337	-2.973	-0.0041	0.0264	2.77062	-0.703	-0.628	-0.459	-0.435	-0.744	-0.694	-0.642	-0.590	-0.560	-0.519	-0.490	-0.462	-0.432	-0.399	-0.391
CENT	AG	4.10	31.2	-0.7615	-0.765	-0.9645	-2.3681	-0.0004	0.02389	1.65094	-0.420	-0.403	-0.308	-0.286	-0.693	-0.640	-0.579	-0.534	-0.500	-0.463	-0.439	-0.410	-0.400	-0.374	-0.354
CENT	AG	5.00	38.0	-1.1133	-1.2695	-1.5355	-3.7314	-0.0011	0.03761	2.22624	-0.607	-0.590	-0.450	-0.420											
CENT	AG	3.60	27.4	-0.3698	-0.3485	-0.4072	-1.0907	-0.004	0.00693	1.40511	-0.263	-0.196	-0.146	-0.145	-0.695	-0.649	-0.587	-0.531	-0.483	-0.463	-0.425	-0.402	-0.369		
EDGE	WG	5.60	42.6	-1.6853	-1.3421	-1.2212	-4.2485	-0.002	0.04231	2.60164	-0.689	-0.619	-0.451	-0.424	-0.694	-0.646	-0.585	-0.538	-0.503	-0.467	-0.438	-0.409	-0.384	-0.345	-0.348
EDGE	WG	6.50	49.4	-1.7085	-0.8656	-0.6886	-3.3207	-0.0012	0.03314	2.8446	-0.650	-0.646	-0.515	-0.487											
EDGE	WG	6.70	50.9	-1.1829	-0.8812	-0.814	-2.8854	-0.0025	0.02716	2.25531	-0.550	-0.569	-0.446	-0.424	-0.732	-0.688	-0.637	-0.586	-0.547	-0.522	-0.497	-0.468	-0.448	-0.428	-0.420
EDGE	WG	6.40	48.6	-1.6061	-0.875	-0.843	-3.3056	-0.0042	0.02988	2.72807	-0.742	-0.718	-0.593	-0.559	-0.712	-0.664	-0.606	-0.557	-0.517	-0.482	-0.457	-0.420	-0.400	-0.377	-0.353
EDGE	WG	5.70	43.3	-1.7739	-1.3318	-1.1021	-4.2685	-0.0022	0.04225	2.64476	-0.746	-0.692	-0.514	-0.472	-0.671	-0.621	-0.560	-0.505	-0.464	-0.413	-0.364	-0.322	-0.278	-0.238	-0.201
EDGE	WG	6.40	48.6	-1.6826	-0.8838	-0.8806	-3.4113	-0.0032	0.03197	2.69388	-0.568	-0.565	-0.444	-0.418	-0.733	-0.687	-0.637	-0.587	-0.551	-0.508	-0.487	-0.456	-0.426	-0.400	-0.393
EDGE	WG	6.30	47.9	-1.5446	-0.8756	-0.6872	-3.1769	-0.0005	0.03232	2.72737	-0.617	-0.592	-0.462	-0.434	-0.731	-0.690	-0.636	-0.592	-0.557	-0.523	-0.489	-0.468	-0.443	-0.426	-0.405
EDGE	AG	5.60	42.6	-3.0477	-1.408	-1.4992	-5.799	-0.0046	0.05664	2.31117	-0.721	-0.685	-0.550	-0.515	-0.657	-0.603	-0.540	-0.484	-0.441	-0.391	-0.348	-0.304	-0.267	-0.216	-0.203
EDGE	AG	6.20	47.1	-0.7342	-1.0722	-1.2483	-2.9343	-0.0024	0.02777	2.27539	-0.496	-0.503	-0.409	-0.388	-0.720	-0.669	-0.612	-0.566	-0.523	-0.489	-0.465	-0.438	-0.401	-0.372	-0.360
EDGE	AG	6.50	49.4	-0.7121	-1.2173	-1.4312	-3.2149	-0.0032	0.02995	2.60533	-0.633	-0.621	-0.449	-0.458	-0.722	-0.671	-0.596	-0.538	-0.483	-0.464	-0.433	-0.405	-0.374	-0.352	-0.338
EDGE	AG	5.80	44.1	-1.0533	-1.3221	-1.6076	-3.7876	-0.0005	0.03888	2.59107	-0.665	-0.630	-0.457	-0.427	-0.713	-0.672	-0.615	-0.566	-0.527	-0.490	-0.462	-0.428	-0.401	-0.373	-0.363
EDGE	AG	5.60	42.6	-0.9709	-1.3809	-1.6689	-3.8217	-0.0048	0.03475	2.45656	-0.826	-0.769	-0.516	-0.499	-0.695	-0.636	-0.563	-0.489	-0.453	-0.436	-0.400	-0.359	-0.335	-0.315	-0.313
EDGE	AG	4.70	35.7	-0.9423	-1.0956	-1.1726	-3.1372	-0.0004	0.03195	1.92013	-0.457	-0.475	-0.369	-0.345	-0.681	-0.635	-0.574	-0.526	-0.482	-0.450	-0.422	-0.404	-0.371	-0.352	-0.323
EDGE	AG	6.40	48.6	-0.6929	-1.2671	-1.4522	-3.279	-0.0012	0.03271	2.85641	-0.697	-0.674	-0.519	-0.491											

Figure 6 - Dimensional change and volume change for NBG-10

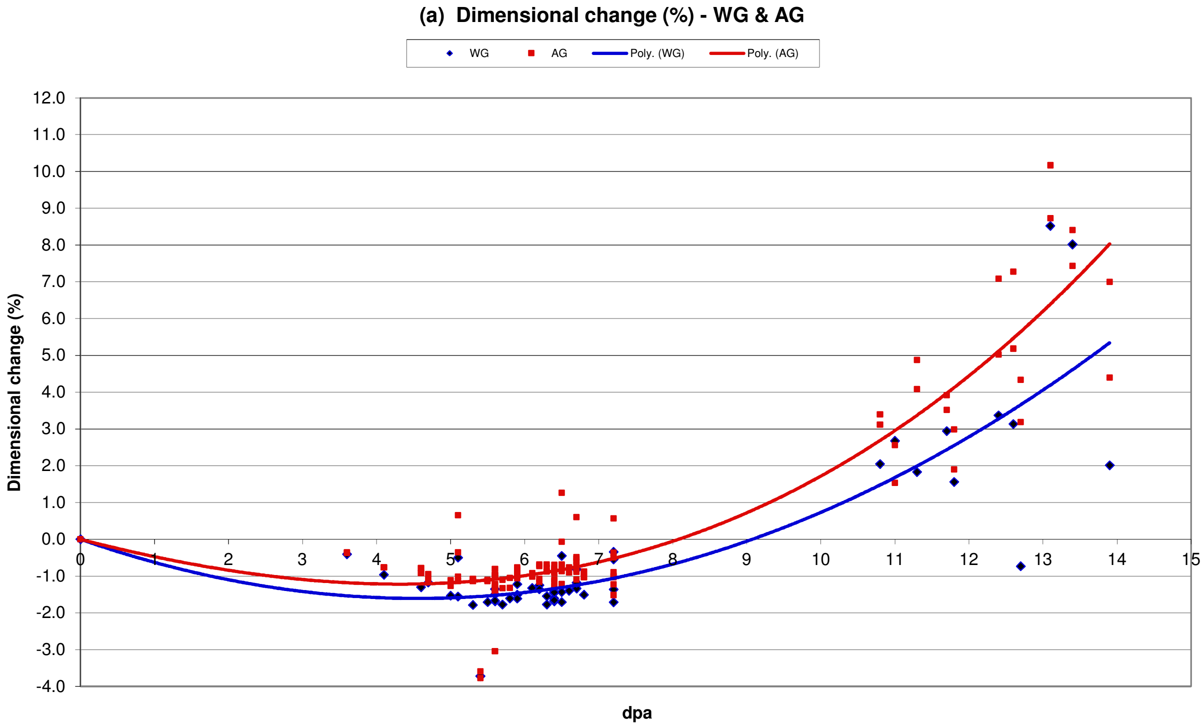

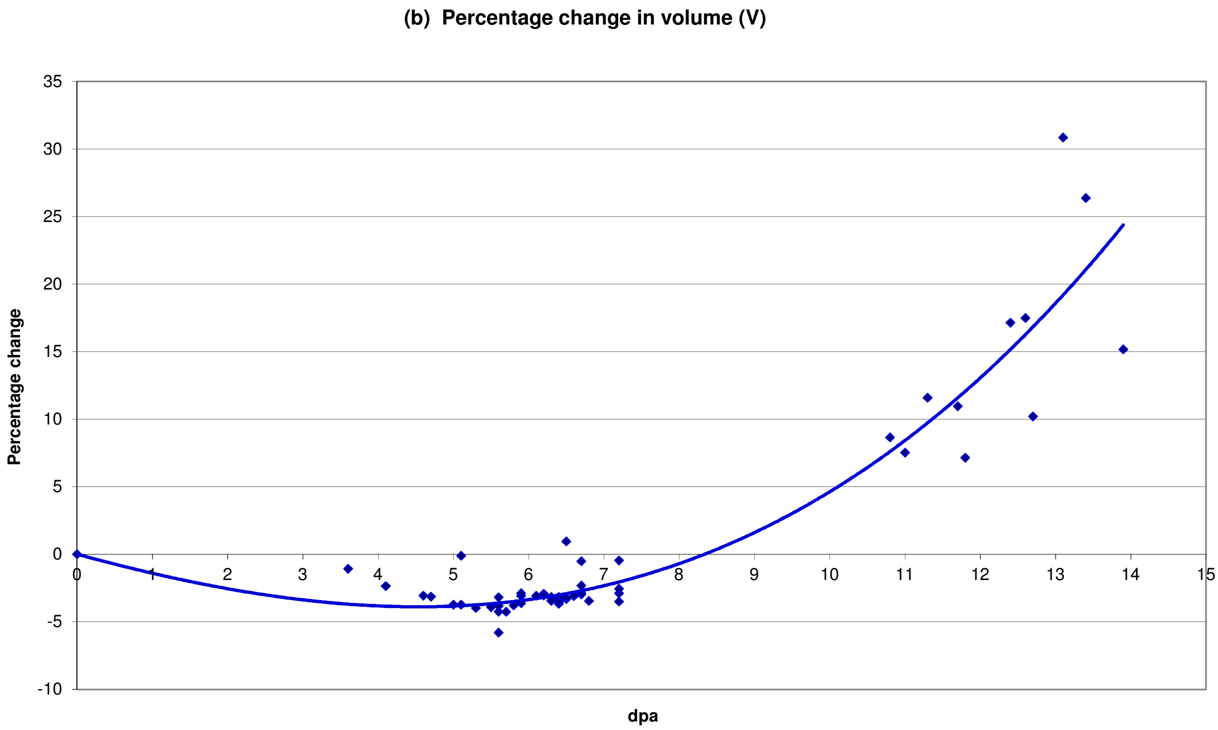

Figure 7 - Dimensional change and volume change for NBG-18

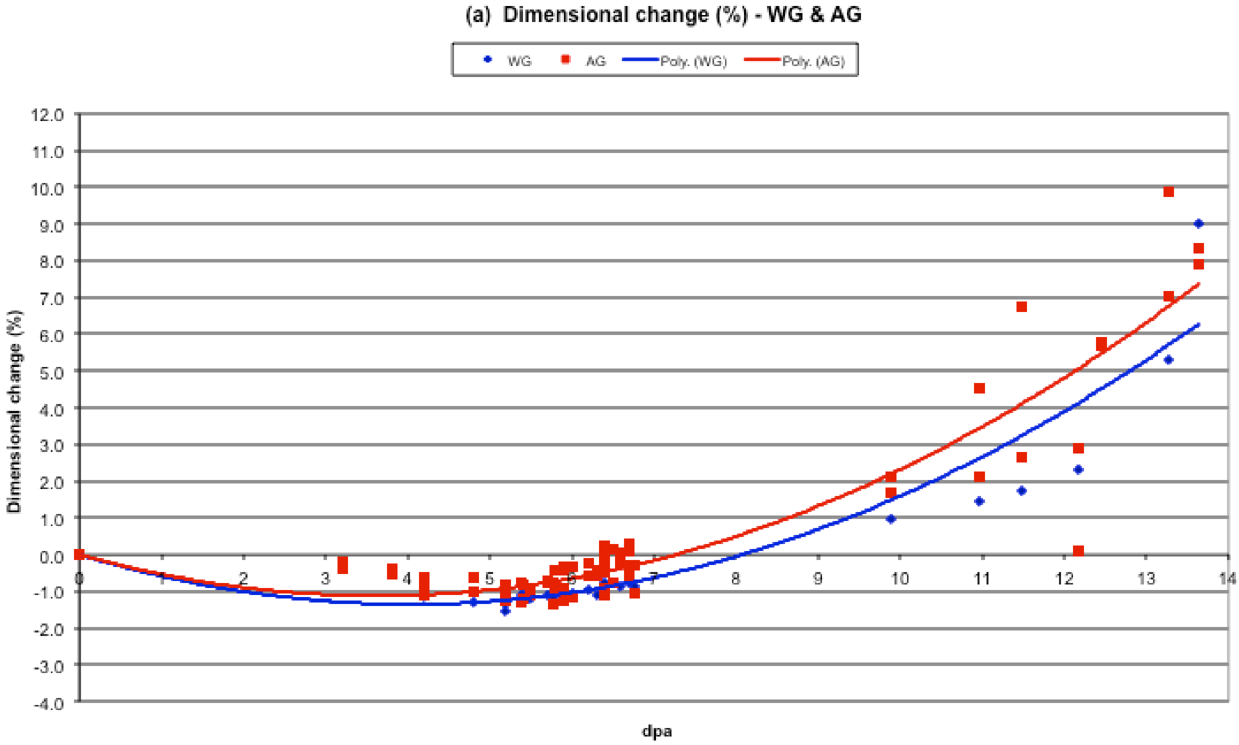

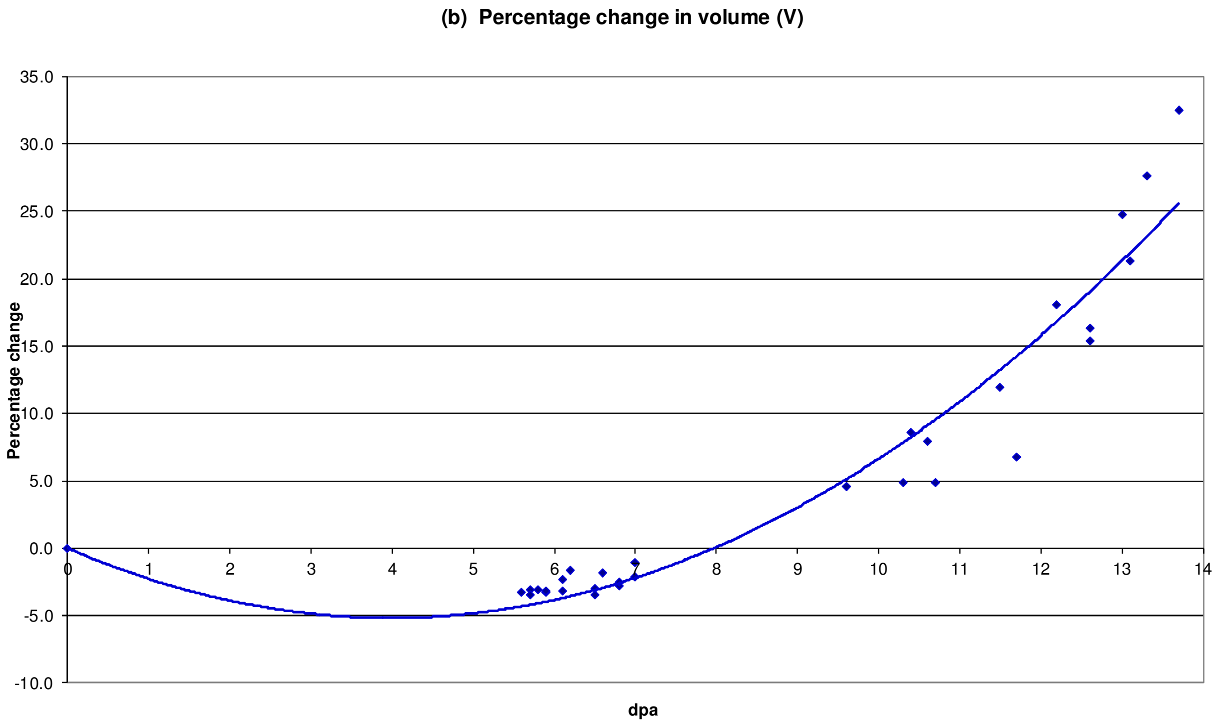

Figure 8 - Dimensional change and volume change for NBG-25

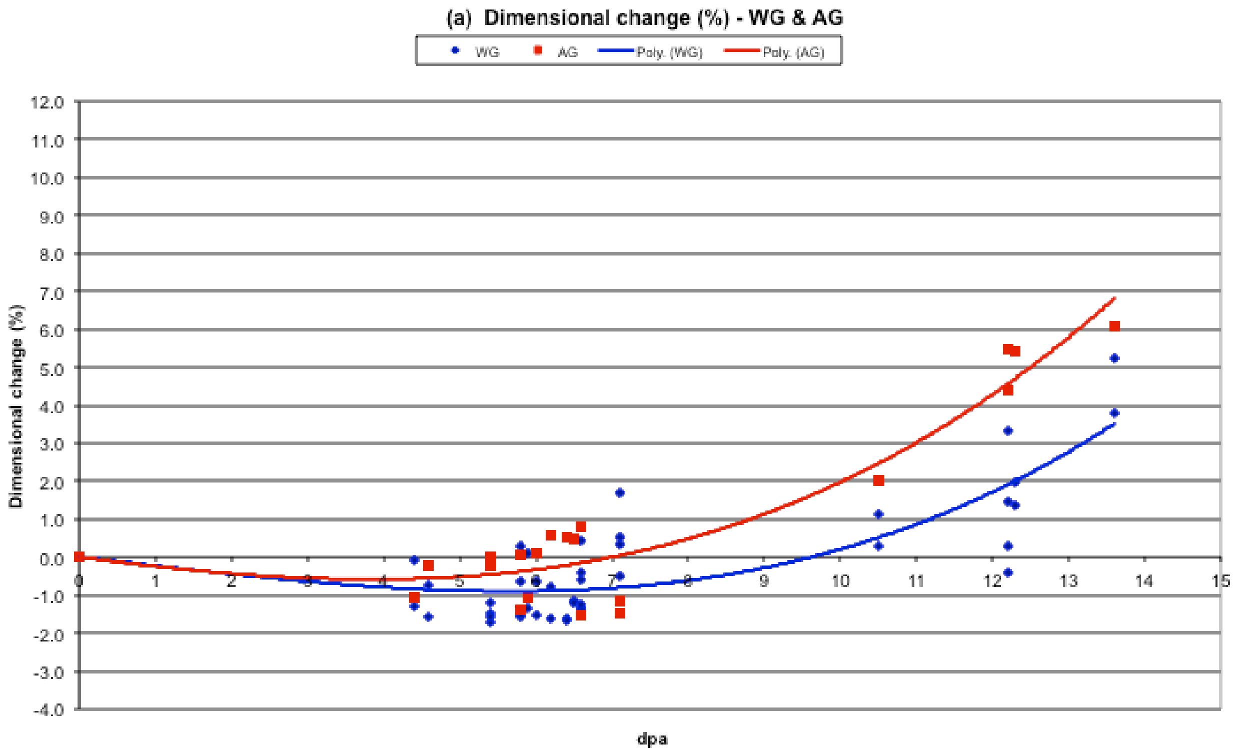

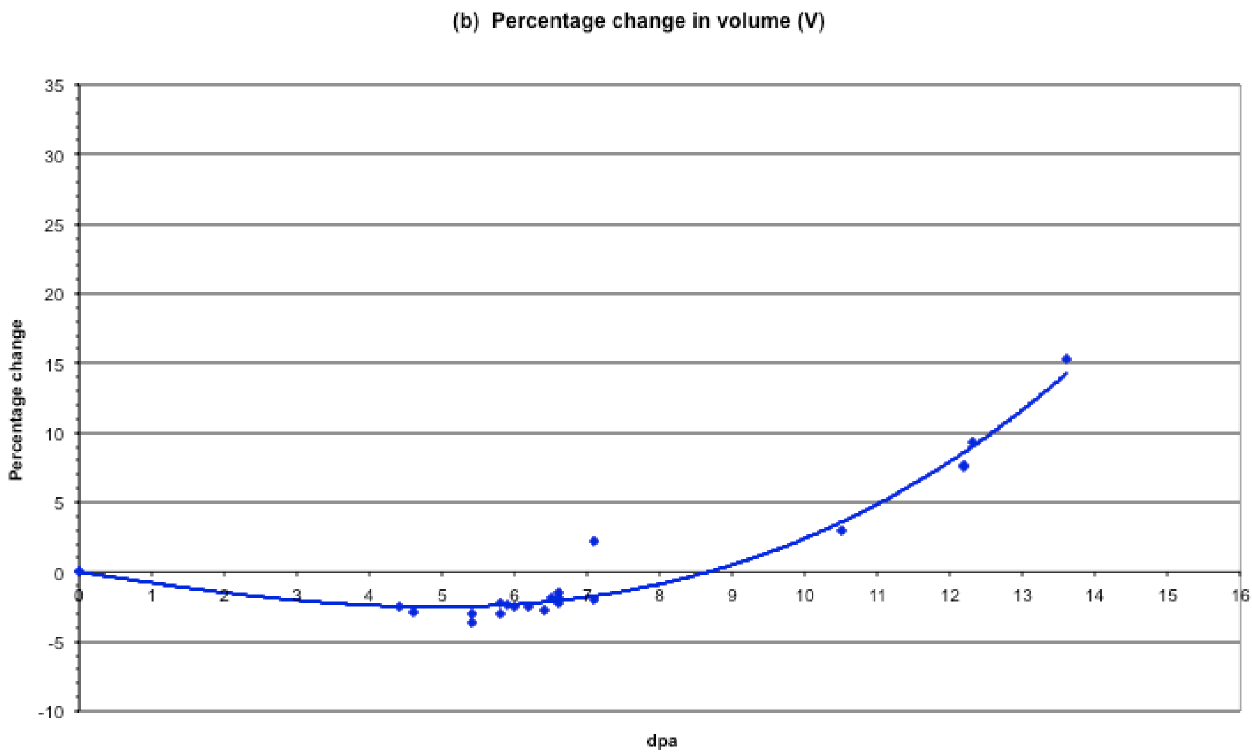

Figure 9 - Dimensional change and volume change for PCEA

(a) Dimensional change (%) - WG & AG

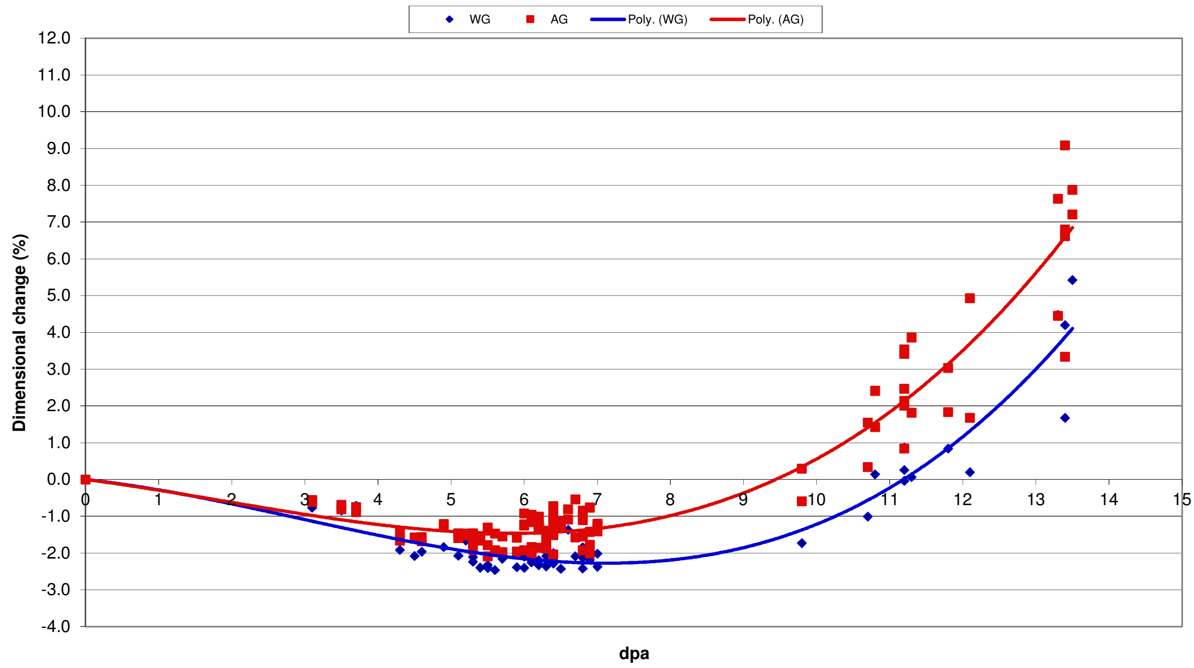

(b) Percentage change in volume (V)

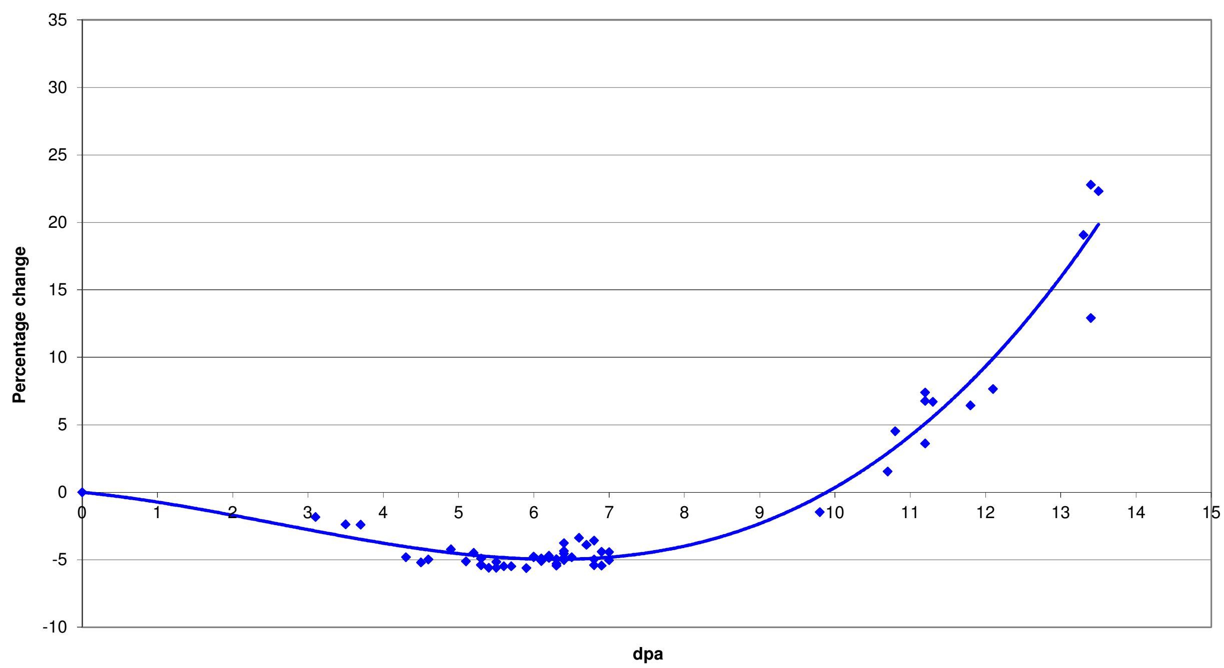

Figure 10 - Dimensional change and volume change for PPEA

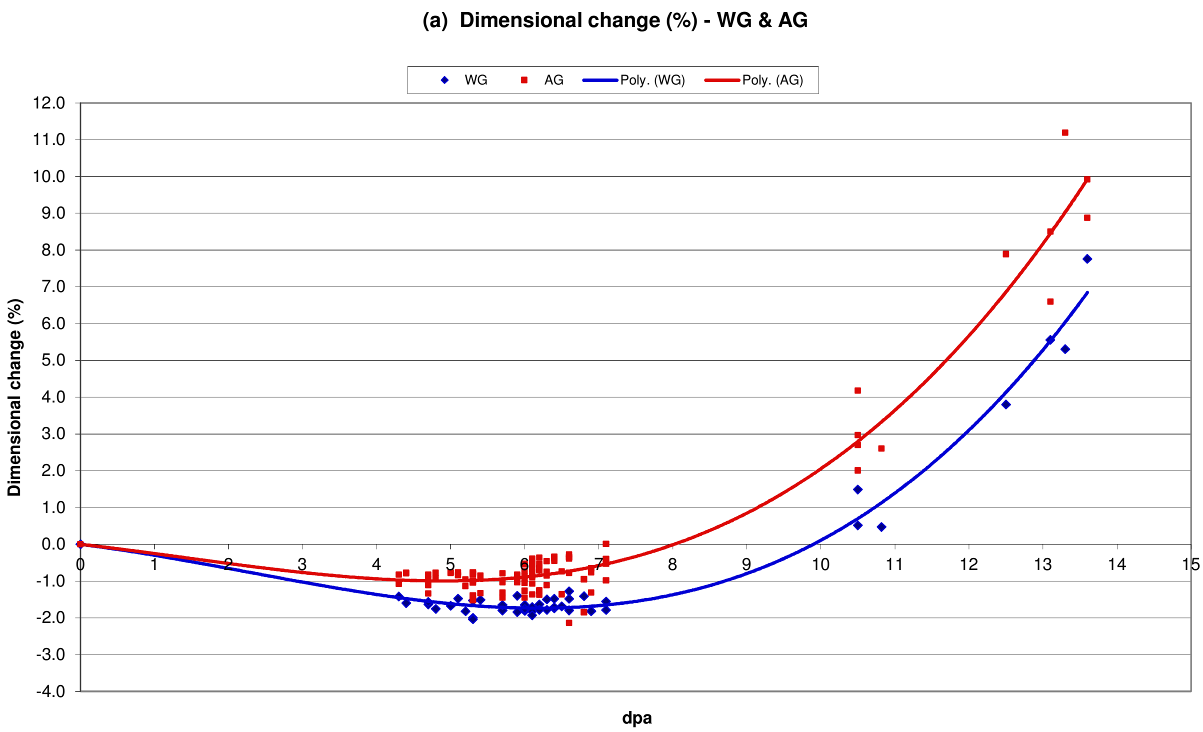

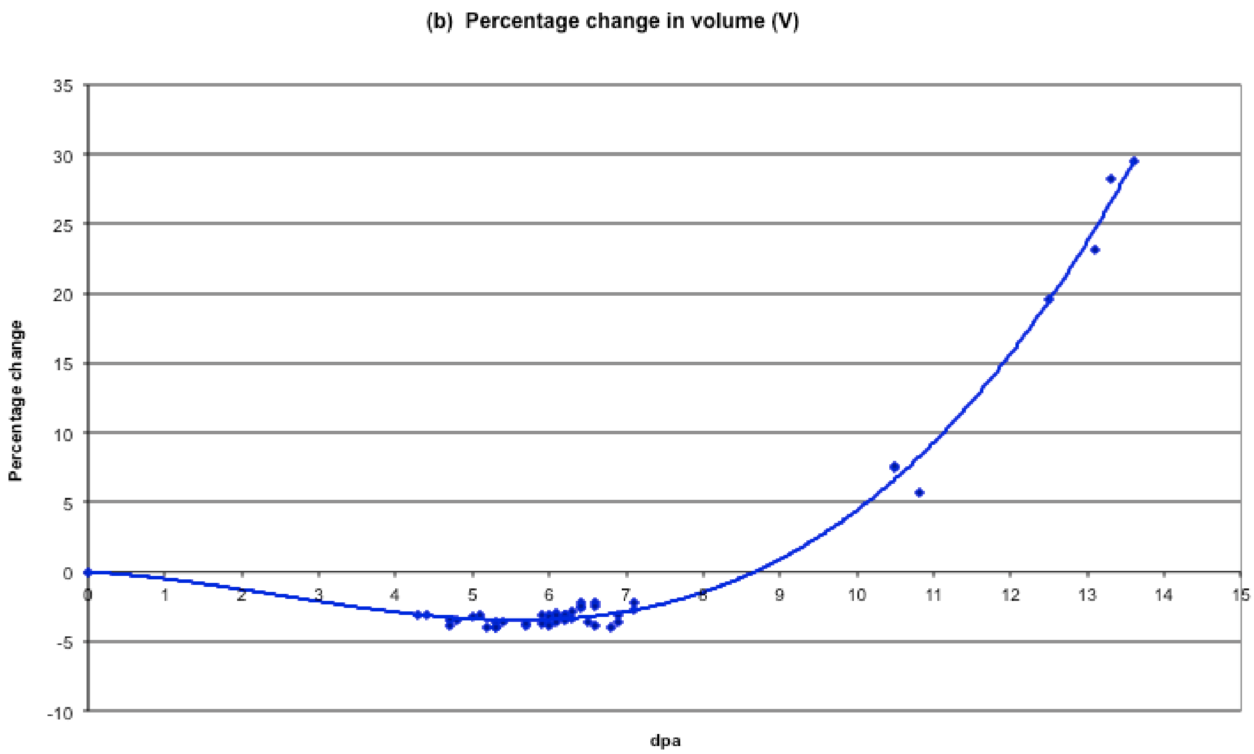

Figure 11 - DYM change for NBG-10

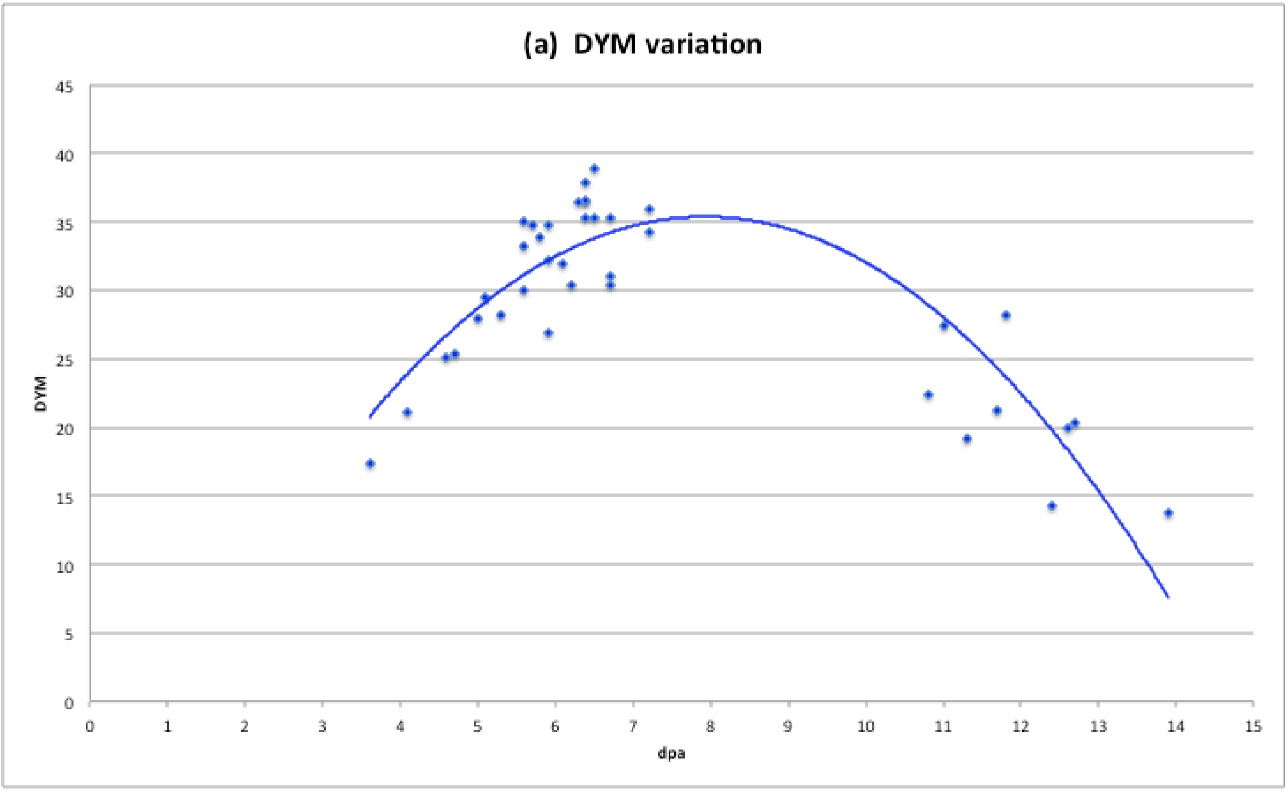

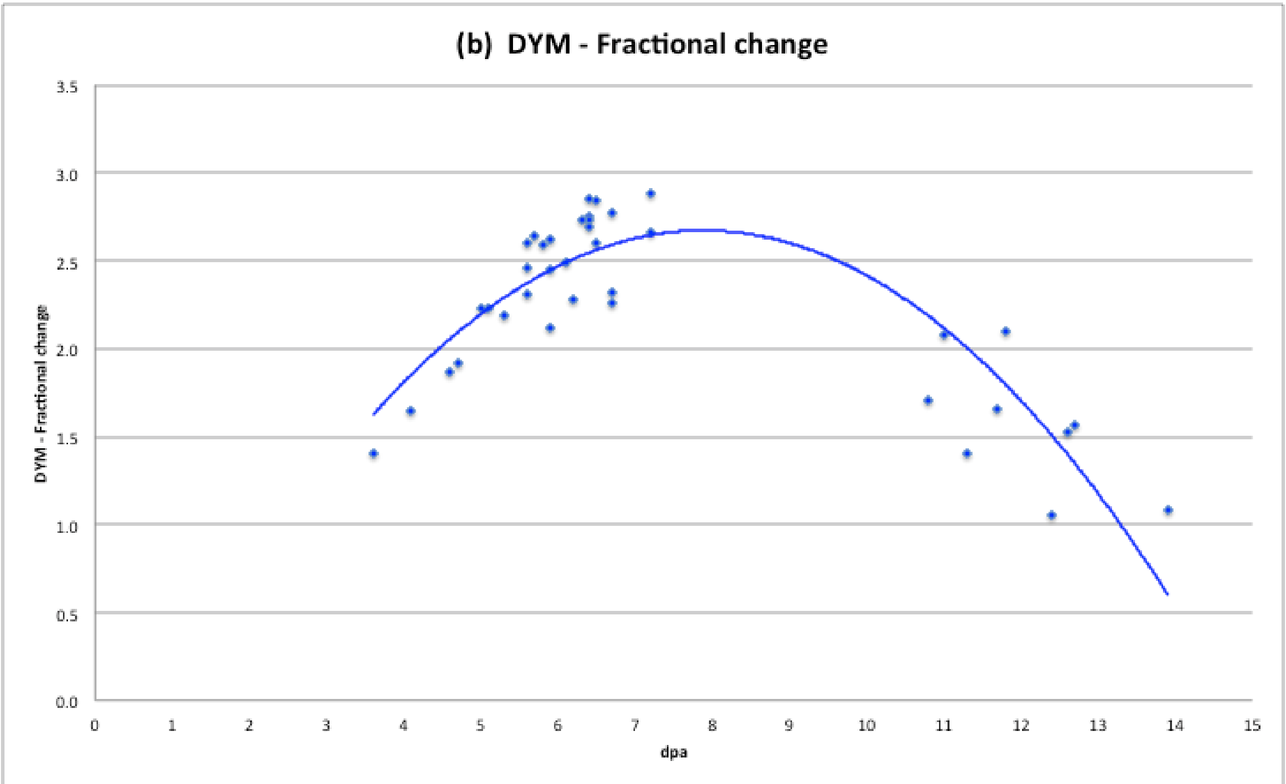

Figure 12 - DYM change for NBG-18

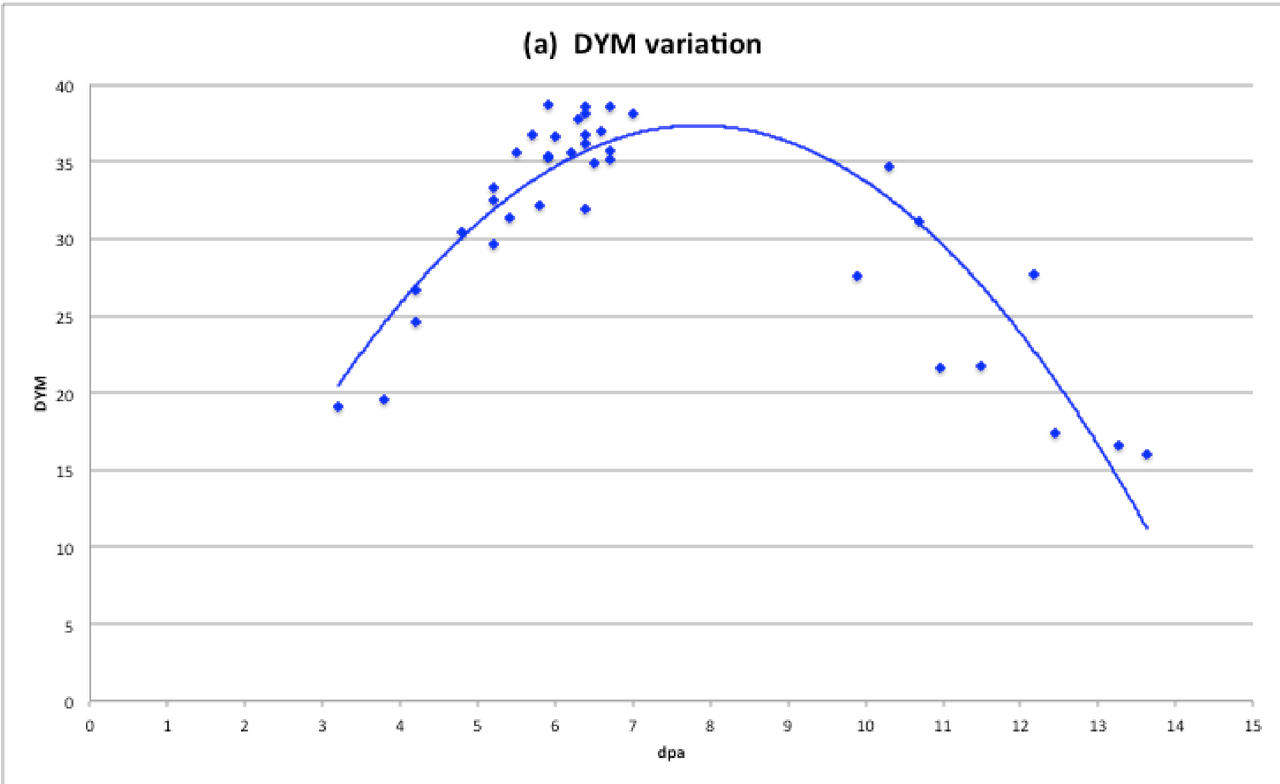

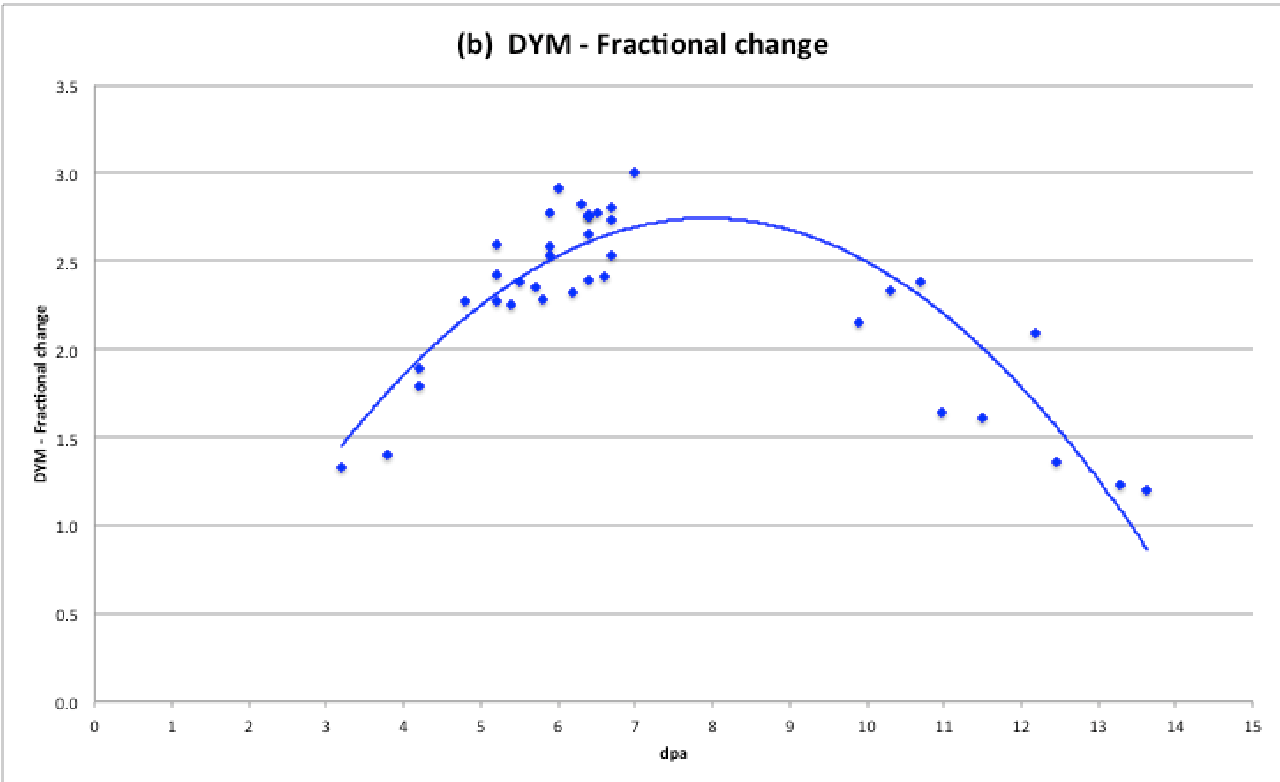

Figure 13 - DYM change for NBG-25

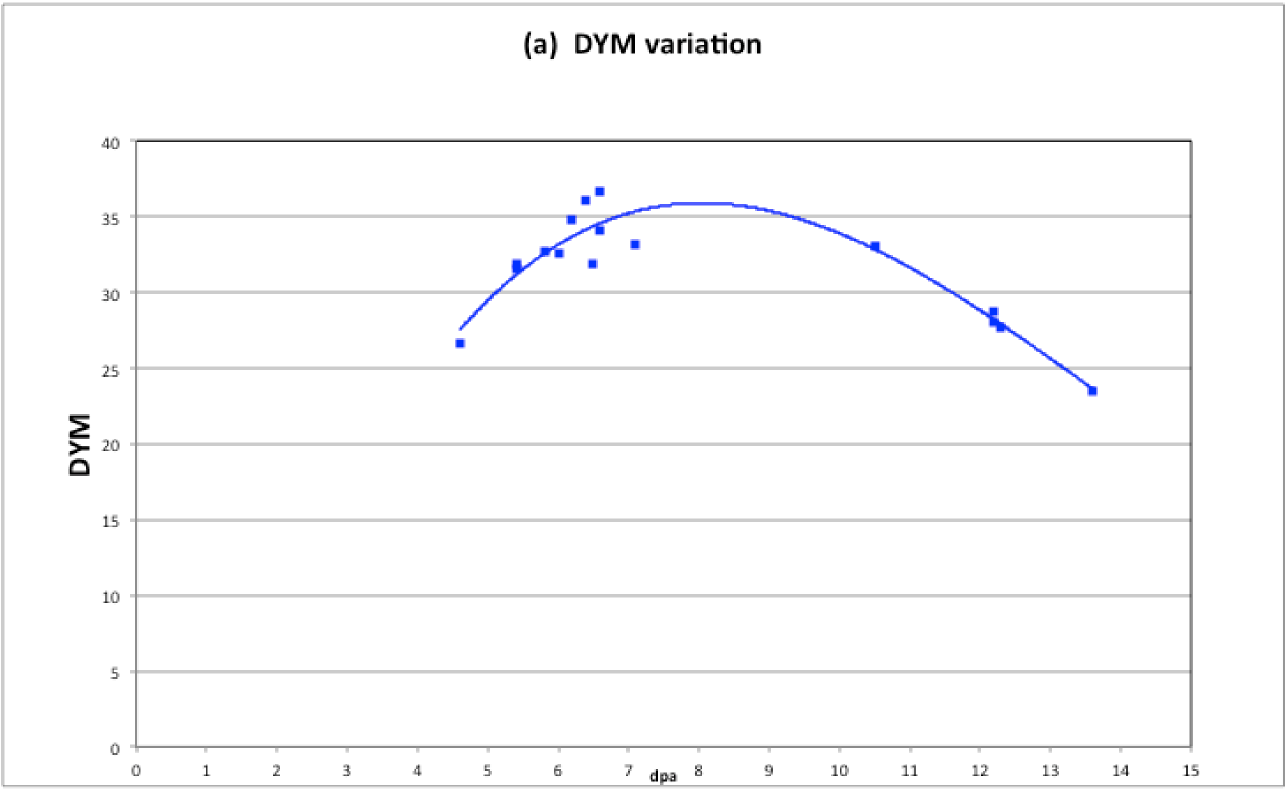

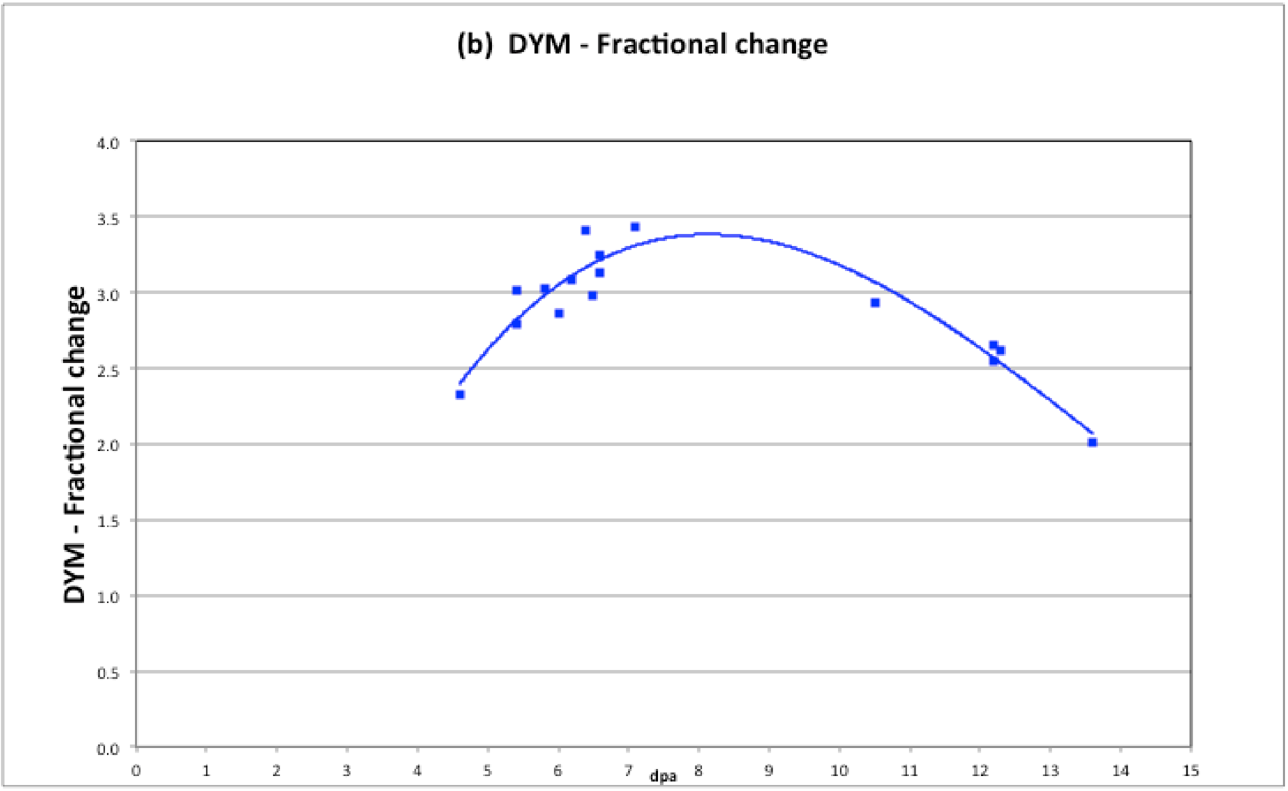

Figure 14 - DYM change for PCEA

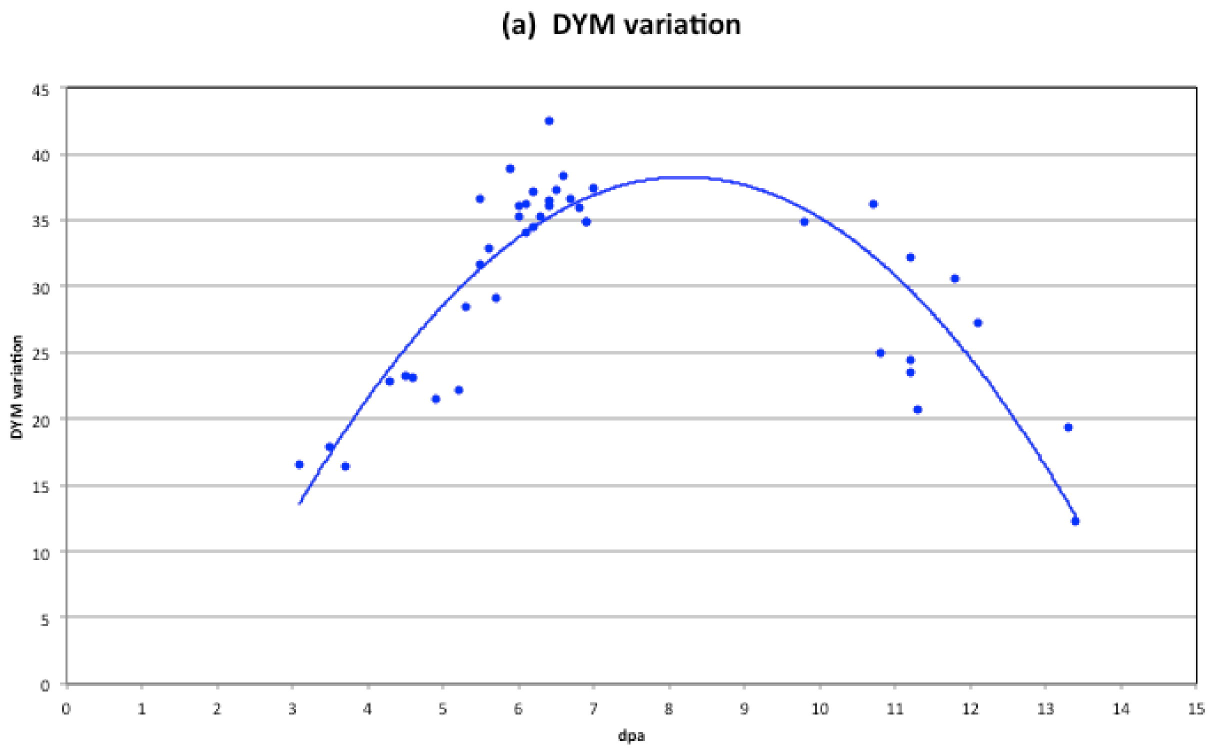

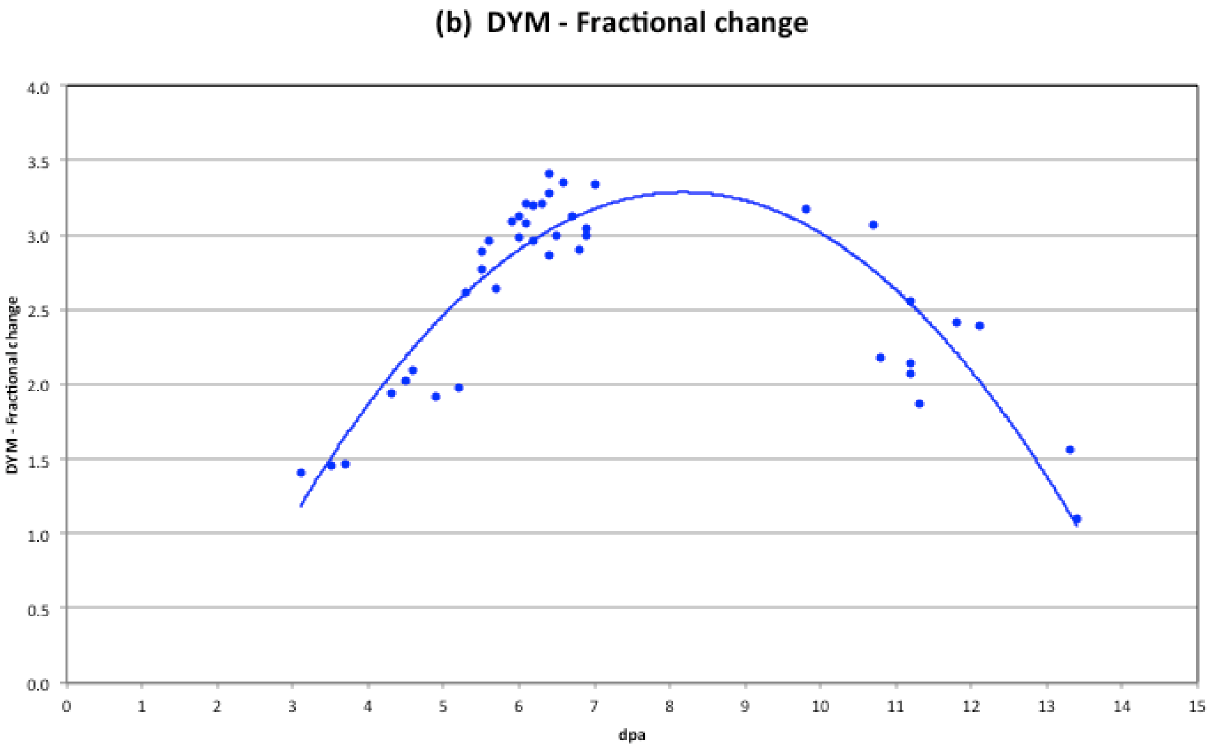

Figure 15 - DYM change for PPEA

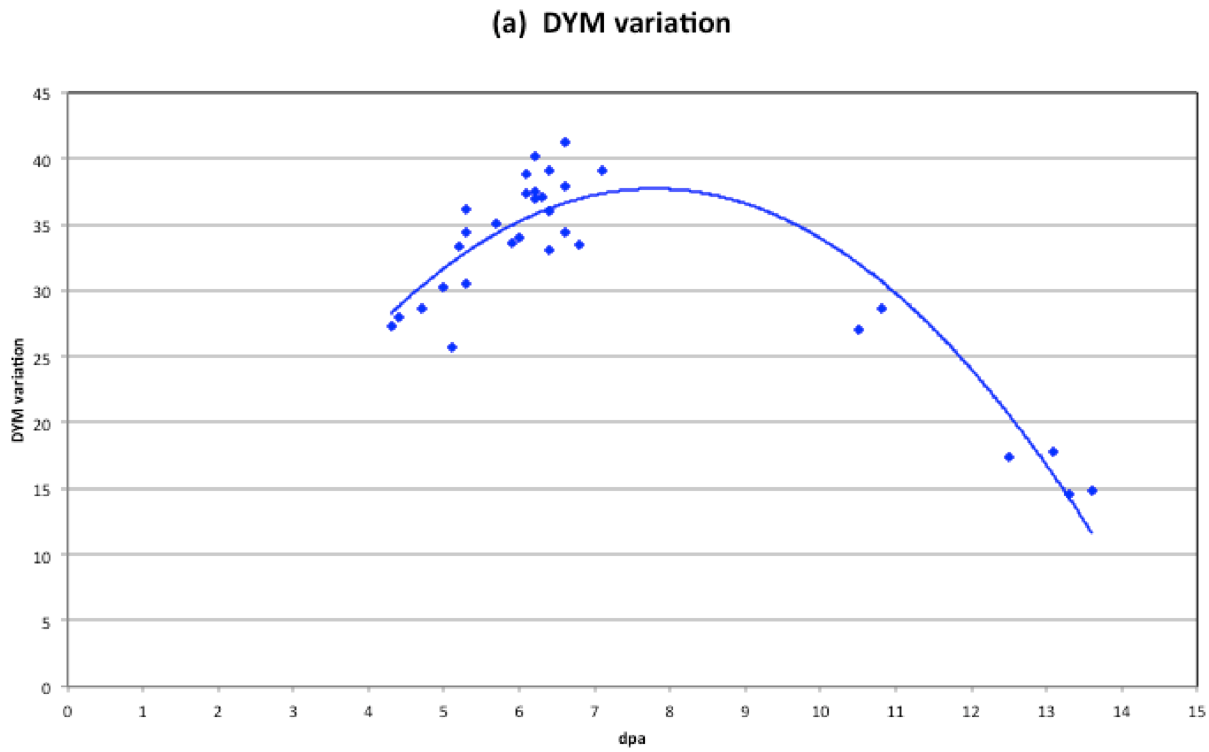

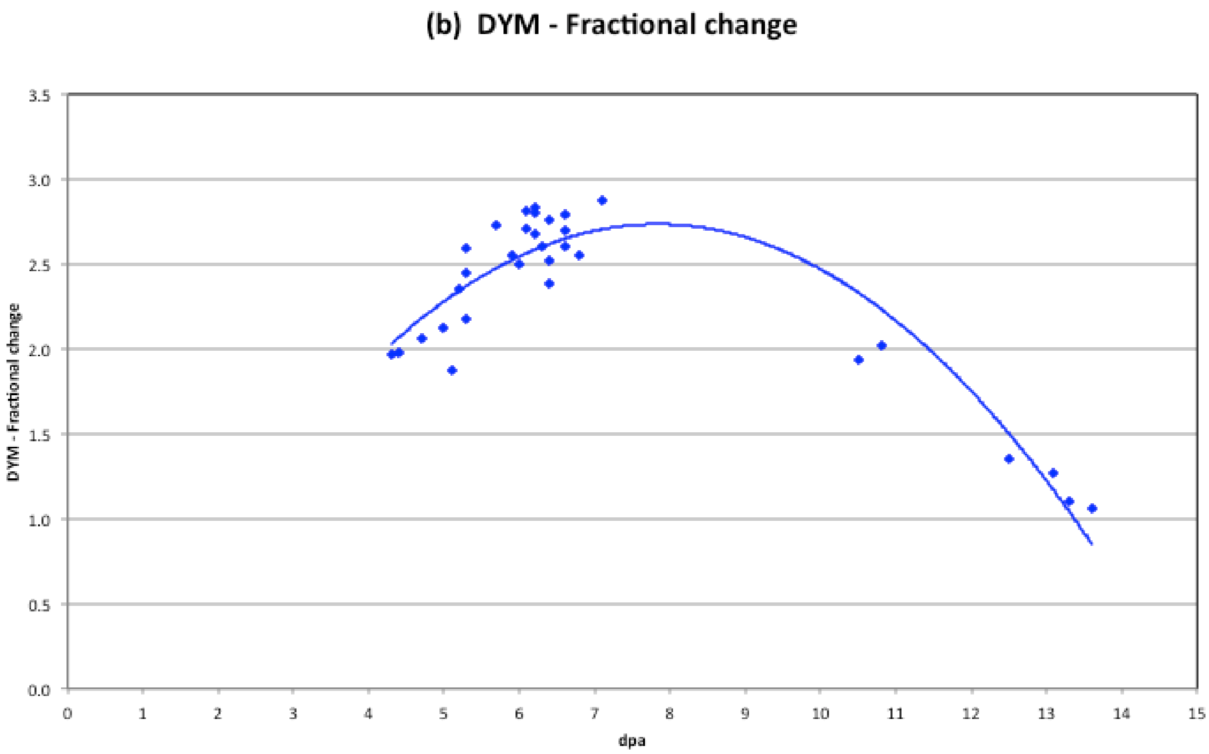

Figure 16 - CTE change for NBG-10

(a) CTE variation

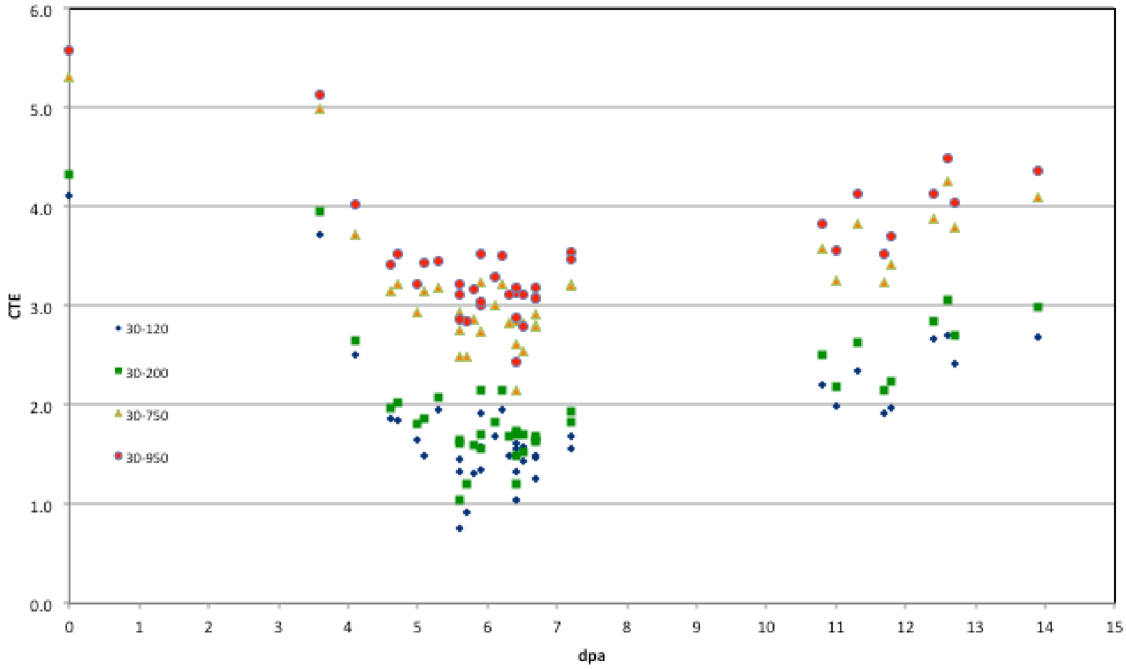

(b) CTE - Fractional change

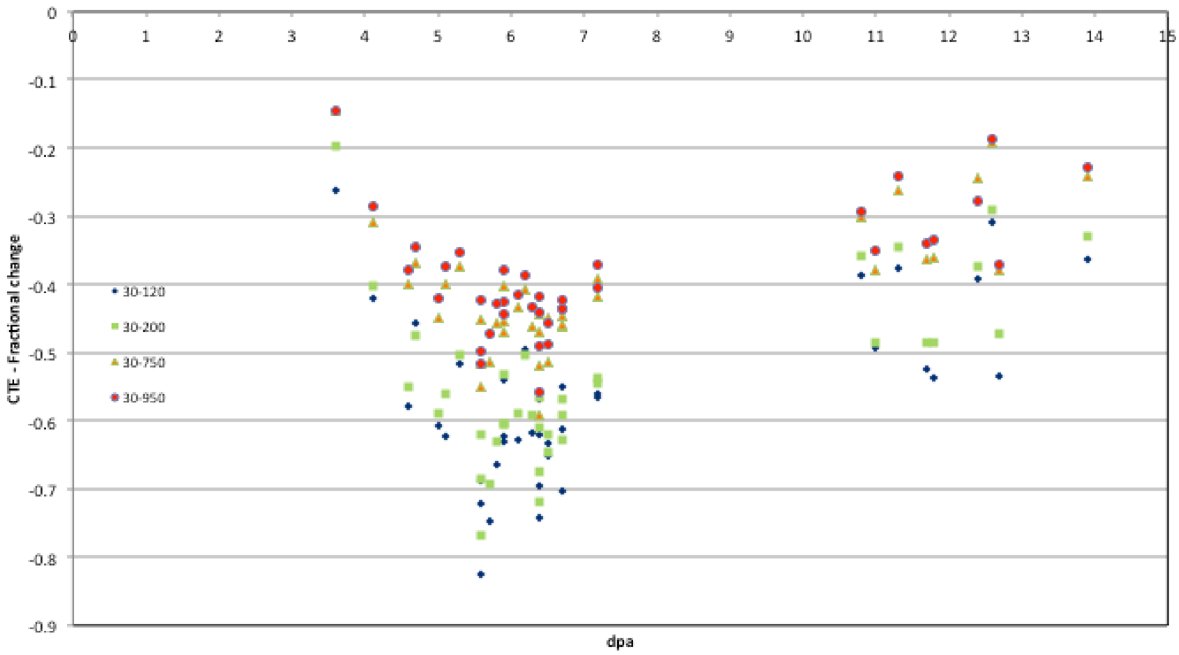

Figure 17 - CTE change for NBG-18

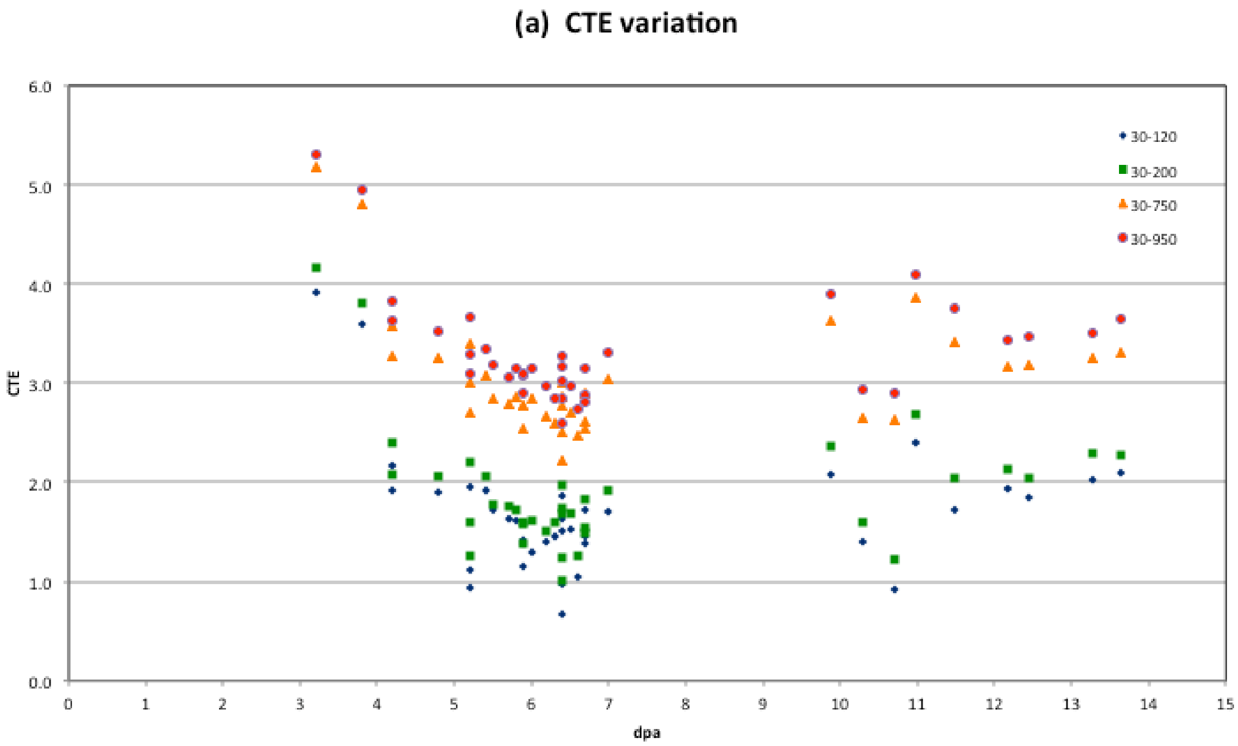

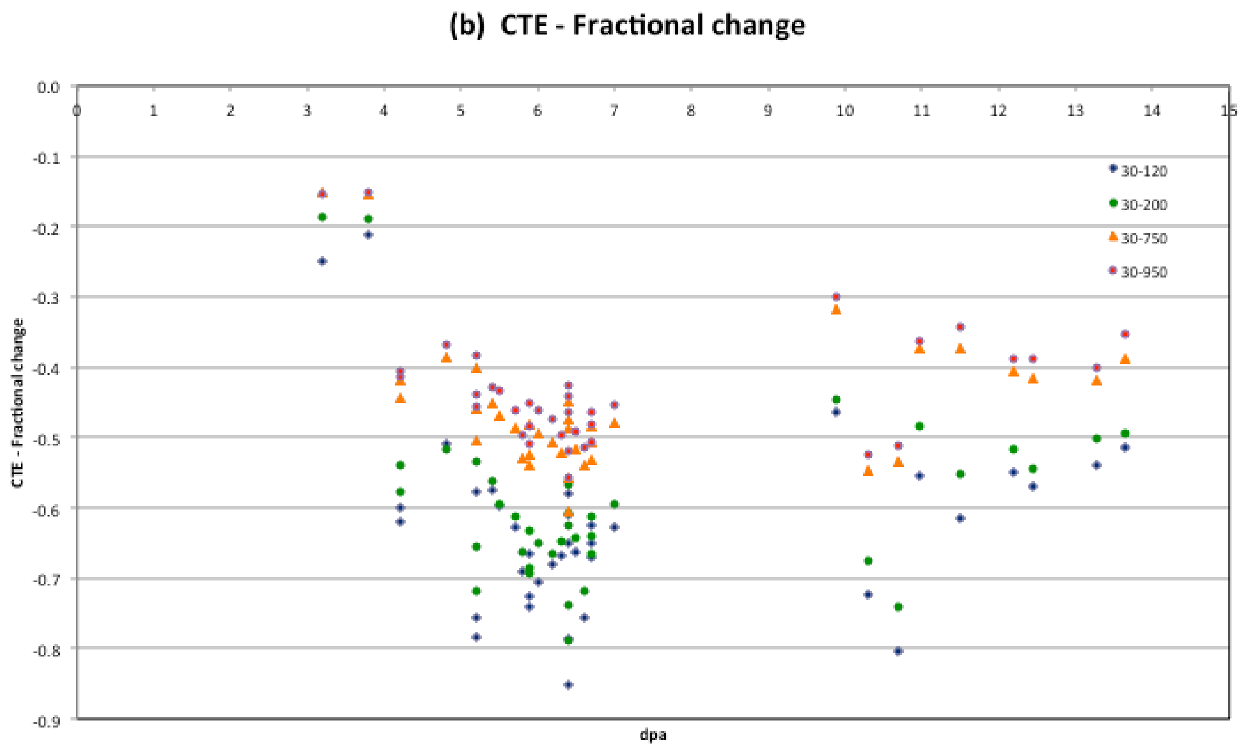

Figure 18 - CTE change for NBG-25

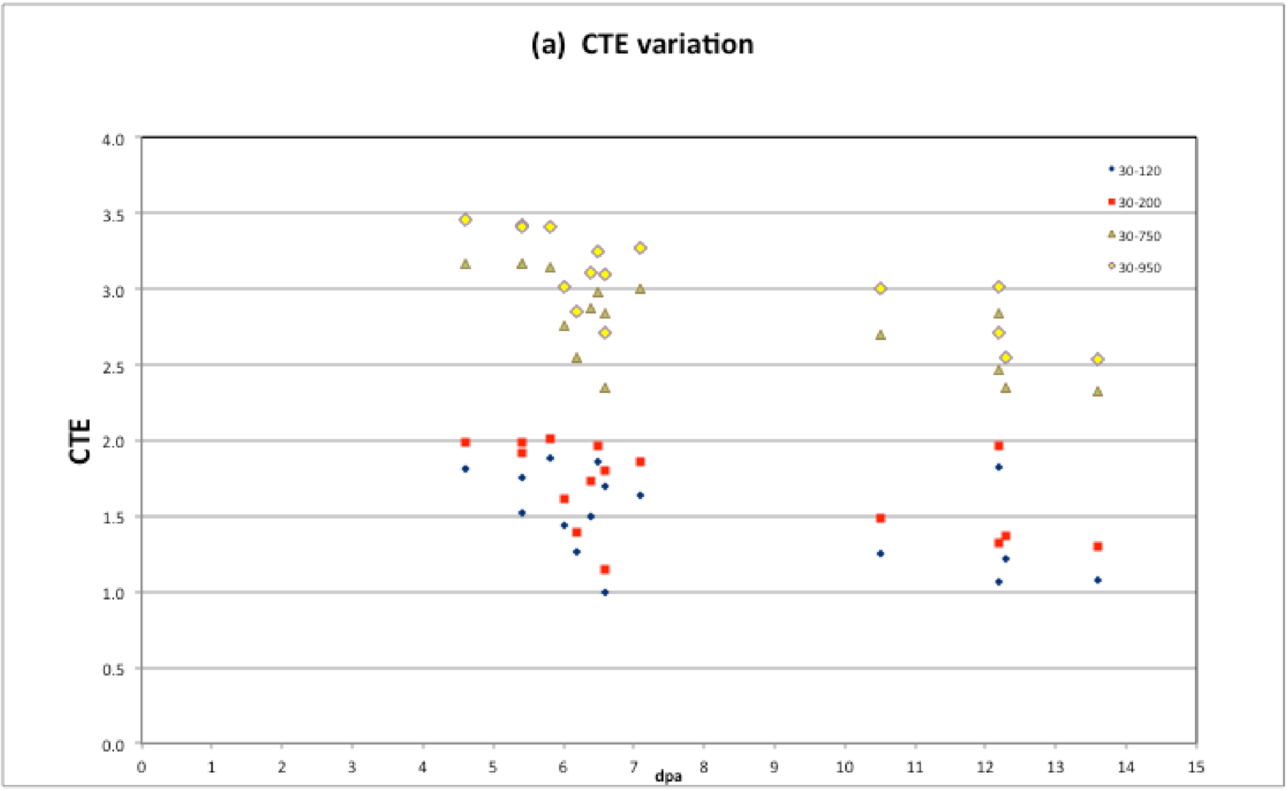

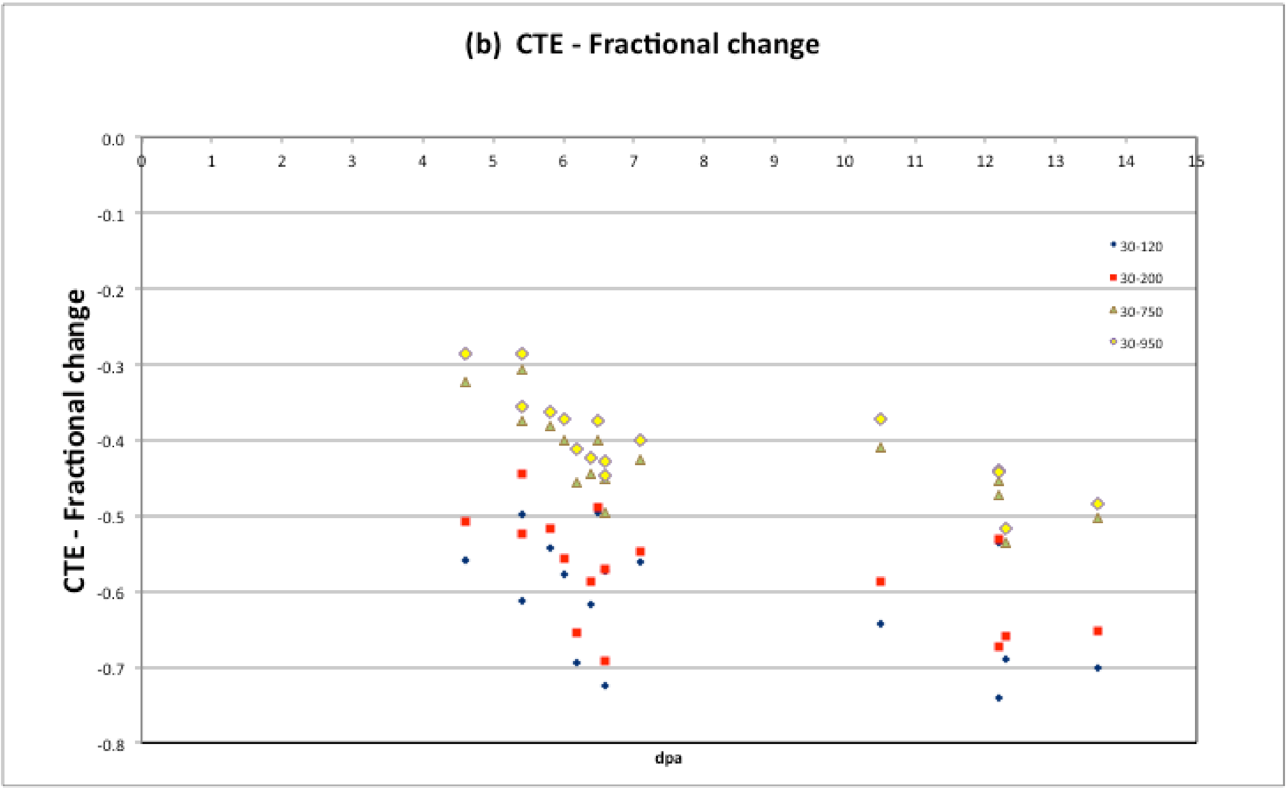

Figure 19 - CTE change for PCEA

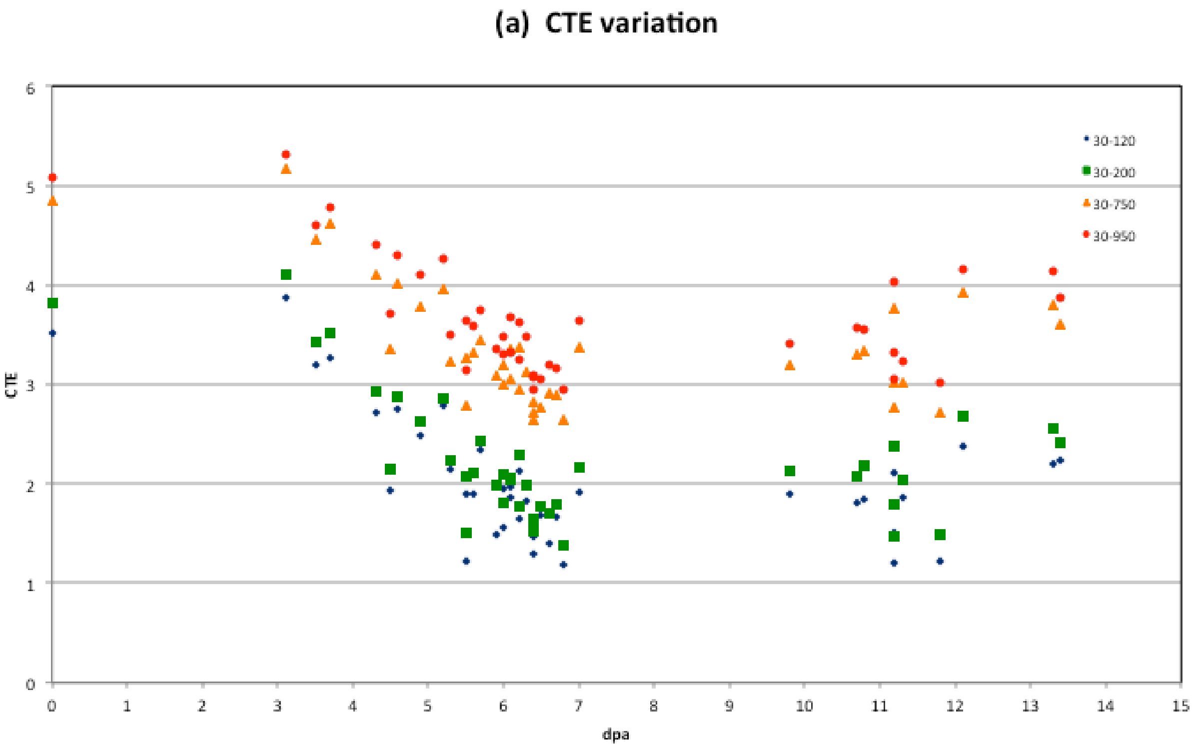

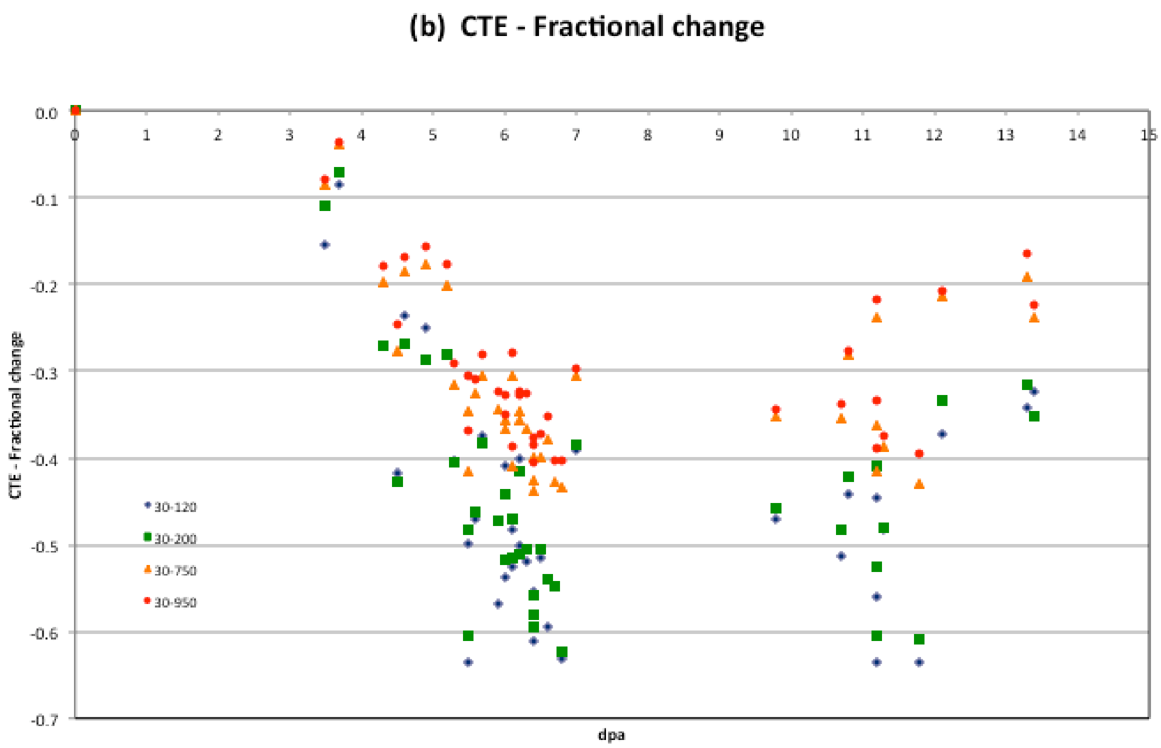

Figure 20 - CTE change for PPEA

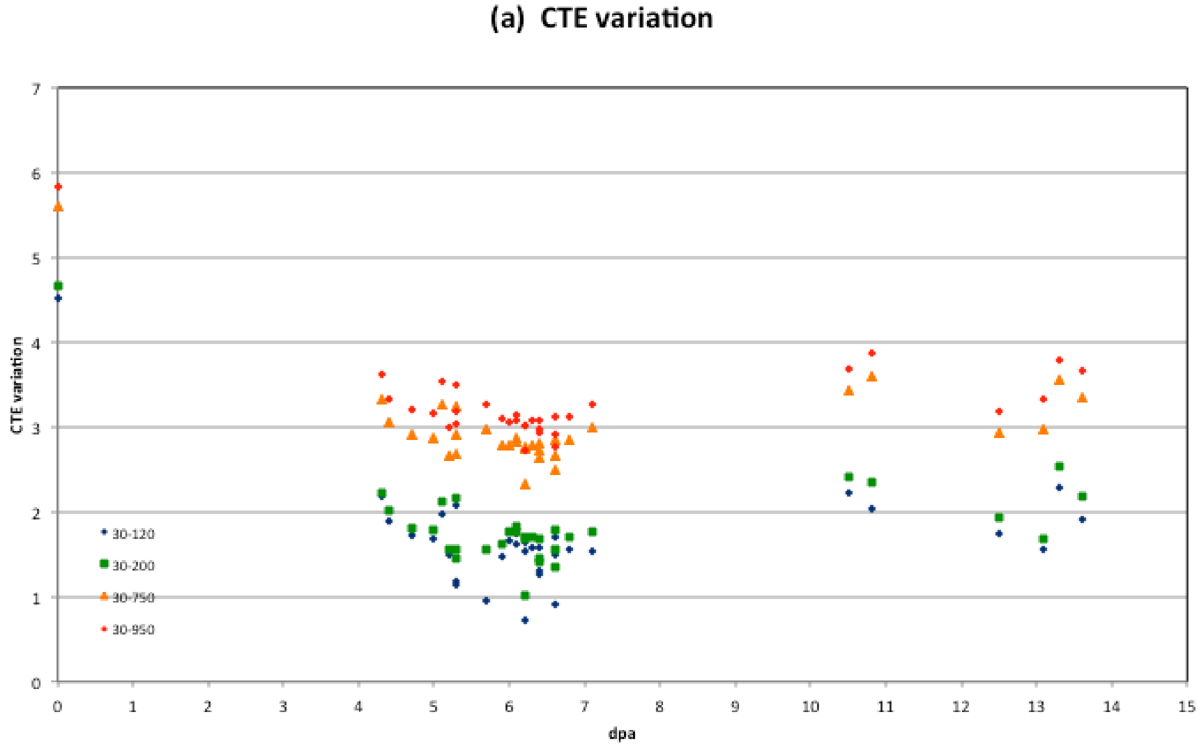

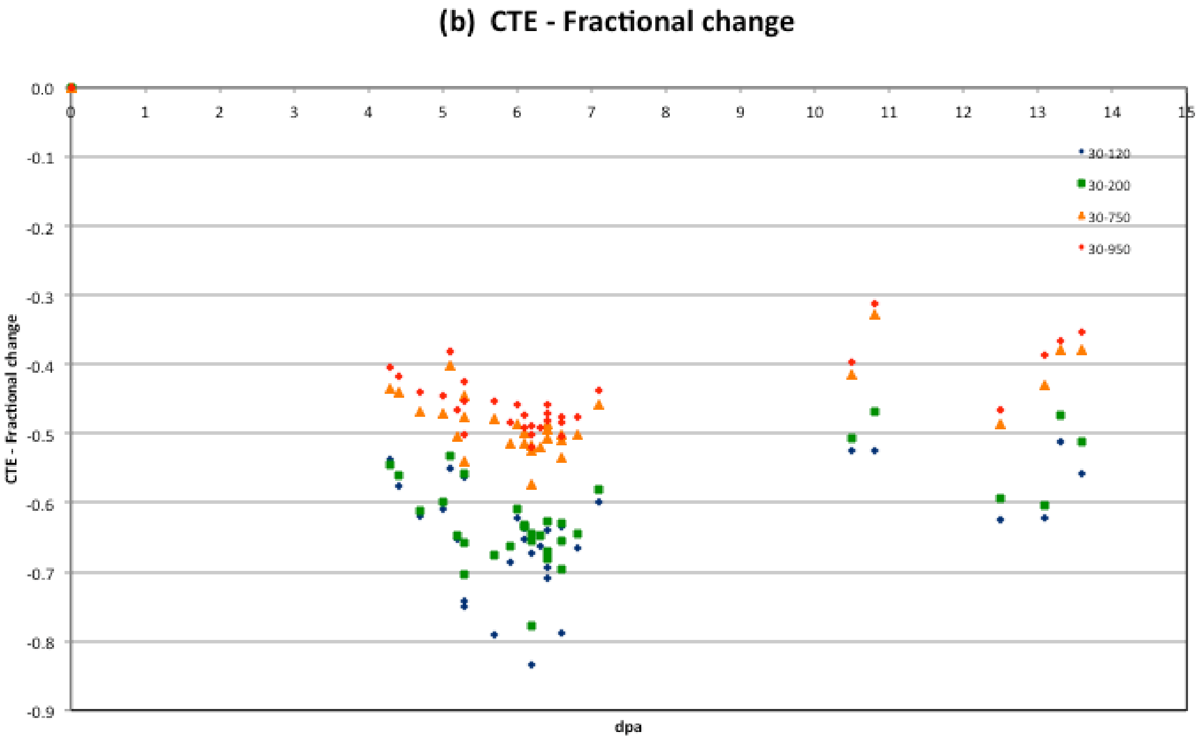

Figure 21 – Thermal conductivity change for NBG-10

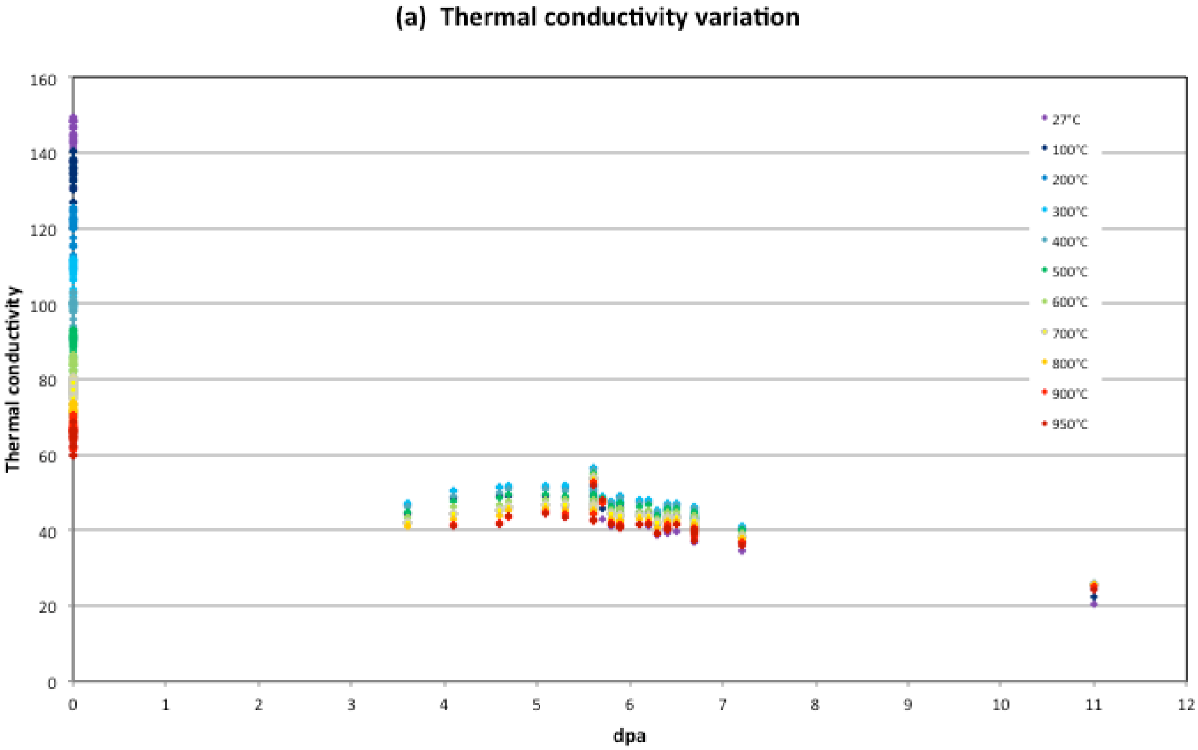

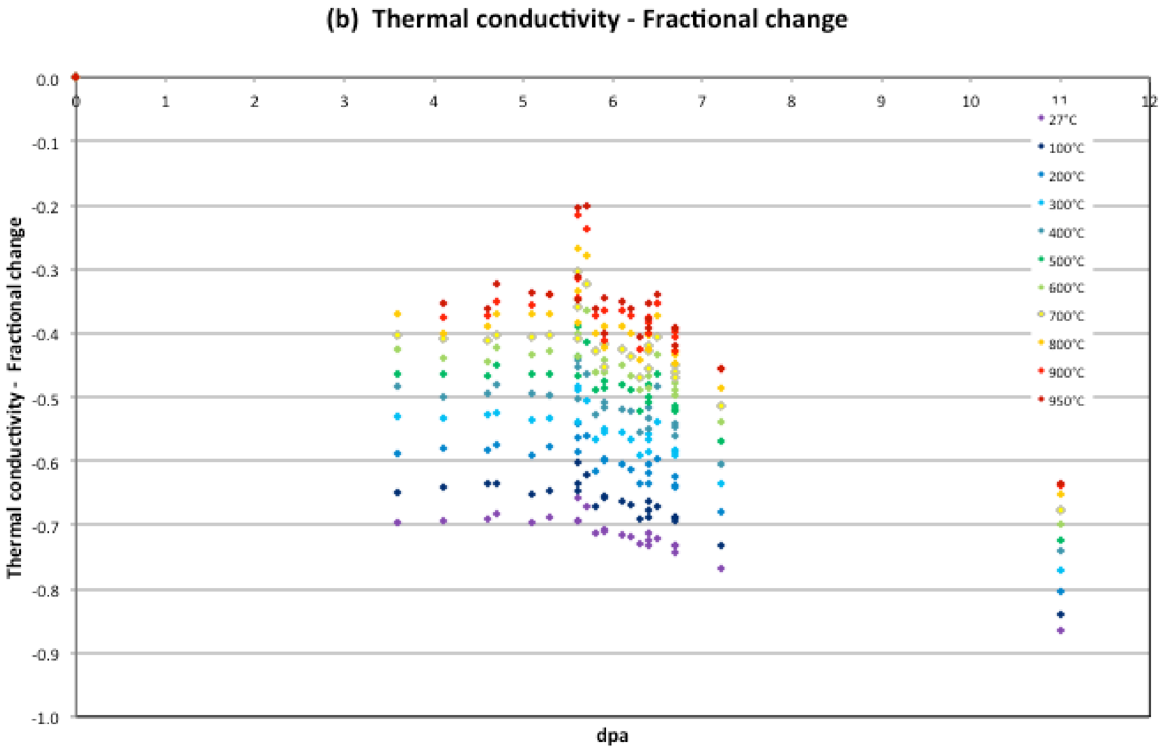

Figure 22 - Thermal conductivity change for NBG-18

(a) Thermal conductivity variation

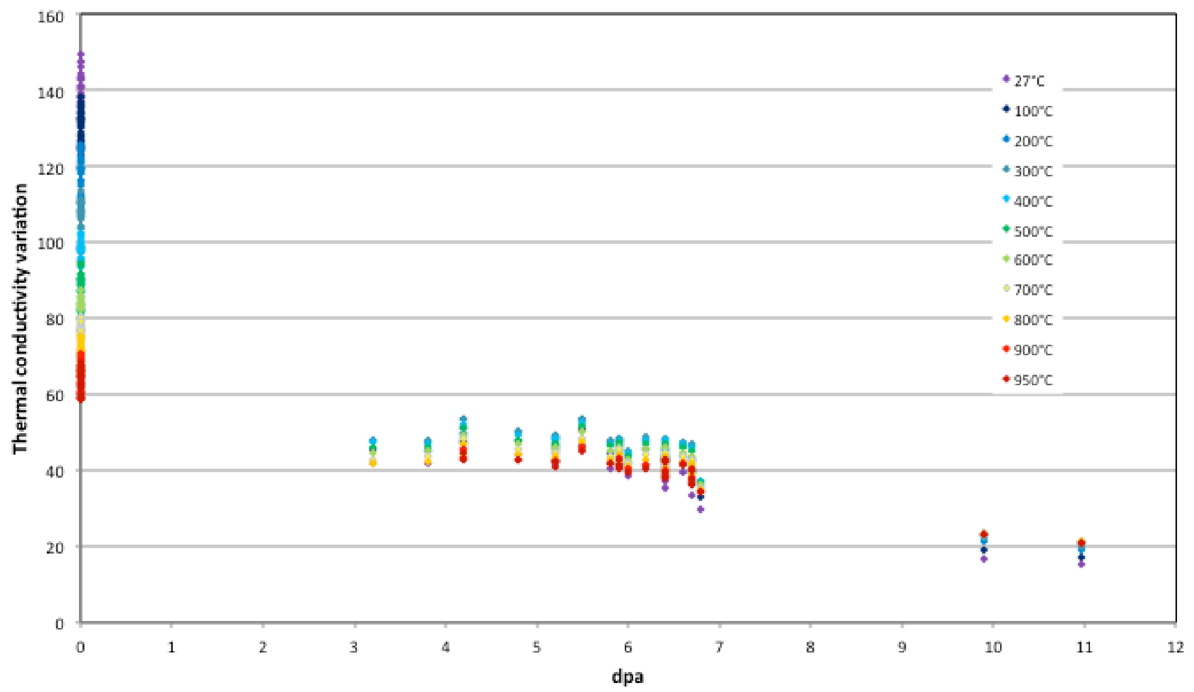

(b) Thermal conductivity - Fractional change

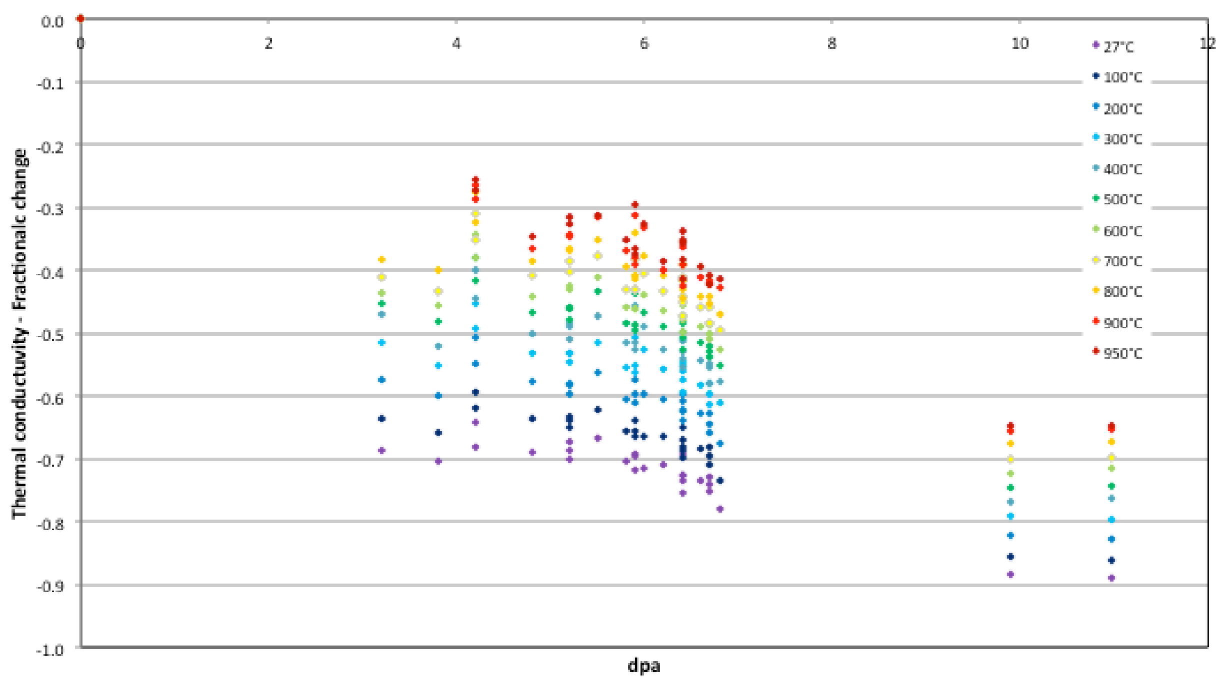

Figure 23 - Thermal conductivity change for NBG-25

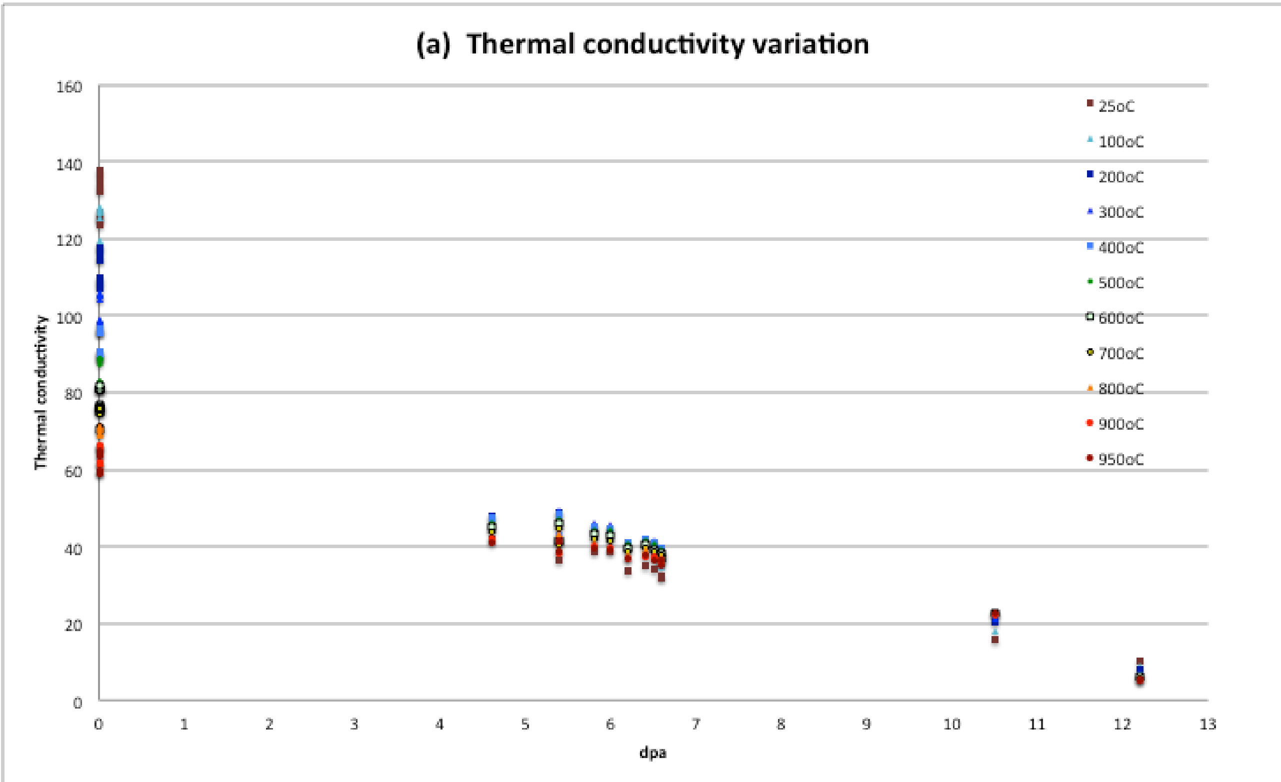

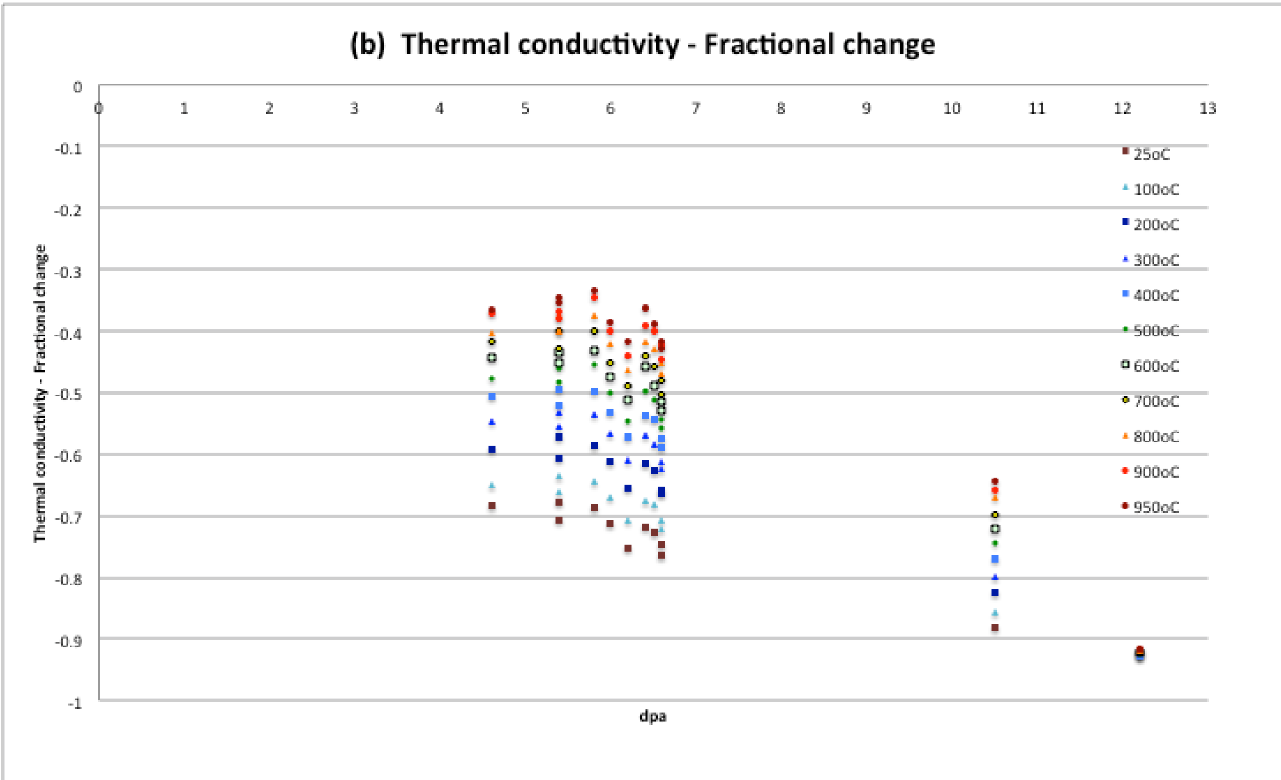

Figure 24 - Thermal conductivity change for PCEA

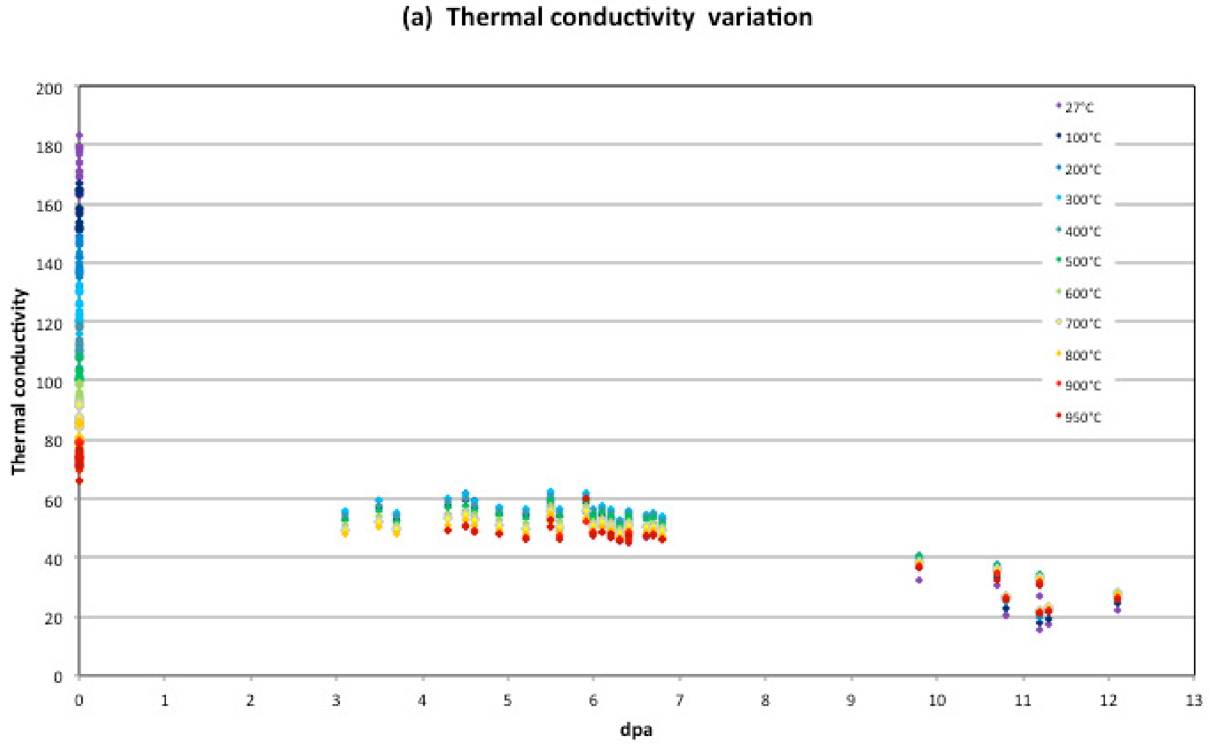

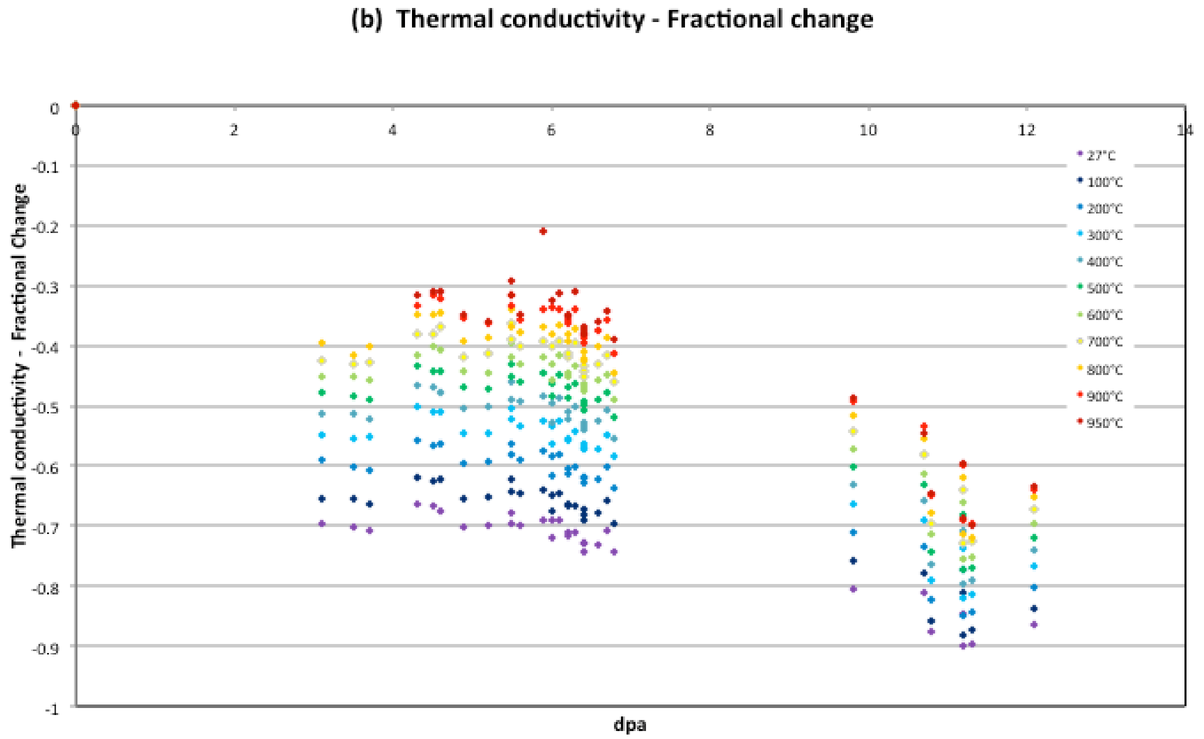

Figure 25 - Thermal conductivity change for PPEA

(a) Thermal conductivity variation

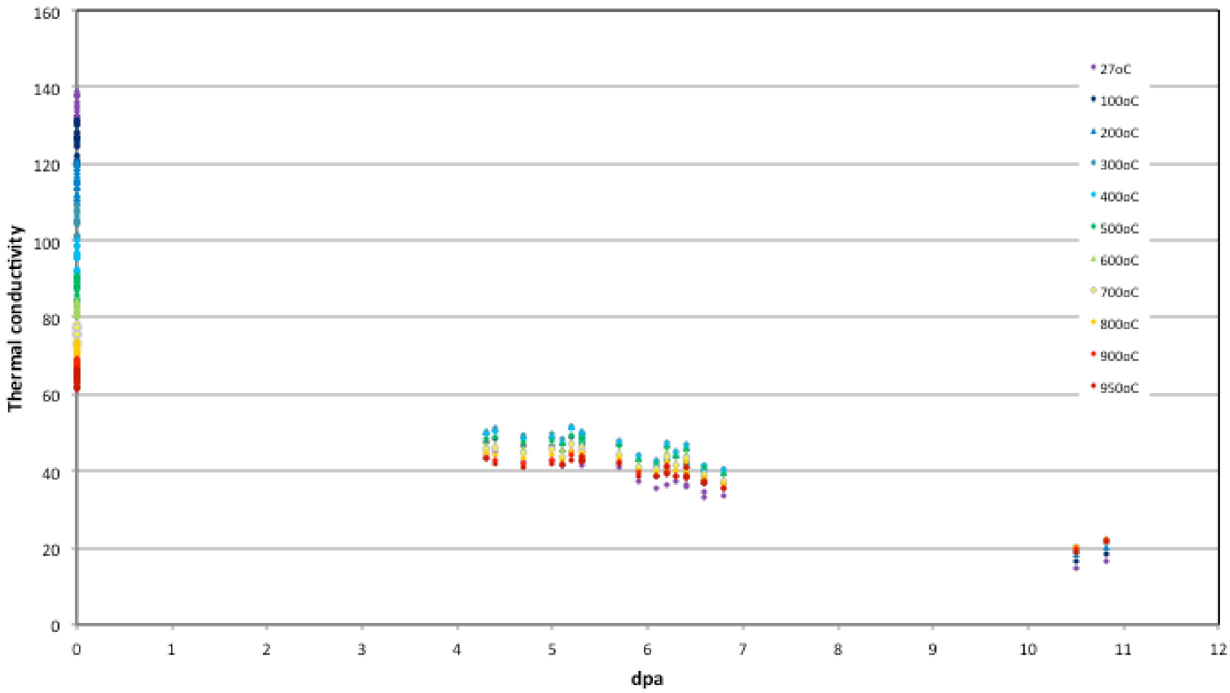

(b) Thermal Conductivity - Fractional Change